Magazine of Civil Engineering. 2020. 93(1). Pp. 97–120
Инженерно-строительный журнал. 2020. № 1(93). С. 97–120

Magazine of Civil Engineering

ISSN 2071-0305

journal homepage: http://engstroy.spbstu.ru/

DOI: 10.18720/MCE.93.9

Strength of underground pipelines under seismic effects

K.S. Sultanov[a]*, J.X. Kumakov[b], P.V. Loginov[a], B.B. Rikhsieva[a]
[a] Institute of Mechanics and Seismic Stability of Structures of the Academy of Sciences of the Republic of Uzbekistan, Tashkent, Republic of Uzbekistan
[b] Tashkent Institute of Architecture and Construction, Tashkent, Republic of Uzbekistan
** E–mail: sultanov.karim@mail.ru*

Keywords: strength, earthquake-resistance, pipeline, soil, interaction, mechanical properties, numerical methods, strain rate, stress

Abstract. A brief analysis of calculation methods to assess underground pipeline earthquake resistance, their advantages and disadvantages are given in the paper. The analysis of the models of underground pipeline-soil interaction under seismic (dynamic) effect is given. The coupled problems of underground pipeline-soil interaction at seismic wave propagation in a soil medium with embedded pipeline are set. One-dimensional non-stationary wave problems for the soil medium and the pipeline are solved numerically using the method of characteristics and the finite difference method. Numerical solutions are obtained in the form of a change in longitudinal stresses over time in various sections of the pipeline. An analysis of the obtained numerical solutions shows a significant dependence of longitudinal stresses on wave processes in the soil medium, dynamic stress state of soil and mechanical properties of soil and the pipeline material. A factor of a multiple increase in longitudinal stresses in the underground pipeline under its dynamic interaction with soil is revealed. It is shown that the main reason for this increase in stresses is the dynamic stress state of soil around the pipeline under its interaction with soil. The results obtained are the grounds for the development of a new regulatory calculation of underground trunk pipeline strength under seismic effect.

1. Introduction

Usage of underground pipelines, which make up some of the most important backbone systems for any population, including water, gas, and oil pipelines, has been on a rise all over the world [1–5]. Their stability under various conditions (seismic ones, landslides, mudflows, transport and sea accidents, etc.) becomes a particularly urgent problem [1–7], since a rise in accident rate of underground pipelines leads to large economic and environmental losses [1]. To prevent this damage, it is necessary to determine the causes of underground pipeline damage under dynamic loads of different nature.

Studies of underground pipeline strength and stability under static and dynamic loads have a long history and have been carried out by many researchers all over the world. The most significant results of the studies are given in [1–9].

Based on the results given in [1–12], the process of the stress state formation, which affects the strength of underground pipelines under dynamic (especially, seismic) loads, is a very complicated one as there are a lot of factors which define the basic determinant indices of this process. Among them are the factors of dynamic (wave) processes in the pipeline itself and dynamic behavior of an underground pipeline depending on its design features [1–4]; the underground pipe-soil interaction factor [1, 13–16]; the factor of surrounding soil with complex mechanical properties [8, 10, 17–31]; the factor of pipelines conveying fluid or gas (thermal and mechanical characteristics) [32, 33]; the factor of dynamic (seismic) load characteristics [32–34], etc. The consideration of all these factors in mathematical statement of the problem leads to complex equations, the solution of which is possible under significant simplifications [32–38]. The attempts to construct generalized models of underground pipeline strain considering complex ground and geological conditions, various models

Sultanov, K.S., Kumakov, J.X., Loginov, P.V., Rikhsieva, B.B. Strength of underground pipelines under seismic effects. Magazine of Civil Engineering. 2020. 93(1). Pp. 97–120. DOI: 10.18720/MCE.93.9

Султанов К.С., Кумаков Ж.Х., Логинов П.В., Рихсиева Б.Б. Прочность подземных трубопроводов при сейсмических воздействиях // Инженерно-строительный журнал. 2020. № 1(93). С. 97–120. DOI: 10.18720/MCE.93.9

of pipe-soil interaction and the effect of corrosive wear on the inside and the outside of the pipe were carried out in [8, 11, 12].

However, determining the qualitative and quantitative impact of each of the above factors is a separate, independent problem in evaluating the underground pipeline strength.

The aim of this study, based on the above factors, is to determine the longitudinal stresses in underground trunk pipelines under longitudinal seismic effects, taking into account the pipeline-soil interaction forces.

The objectives of the paper are:

1. An analysis of existing methods for determining longitudinal stresses under seismic effects.

2. A development of the models of underground pipeline-soil interaction.

3. The statement of the problem of longitudinal underground pipeline-soil interaction under plane seismic waves.

4. The method of solution of wave problem and its substantiation.

5. Comparative analysis of longitudinal stresses in an underground pipeline at various models of pipeline-soil interaction under seismic loads.

2. Methods

2.1. Methods to determine longitudinal seismic stresses in underground pipelines

Currently, there are three basic methods to determine longitudinal seismic stresses in underground pipelines. As described in [9] the first method is based on the hypothesis of the equality of longitudinal strains in the pipeline and soil under seismic loading. Here, the seismic load is taken in the form of plane elastic wave propagating in soil, changing according to a sinusoidal law. Such a statement allows analytical determining the maximum elastic strain in soil [9]. It is assumed that an underground long pipeline receives the strain equal to the maximum elastic strain of soil. Longitudinal stress is determined from Hooke's Law at a known longitudinal pipeline strain. This simple method is laid as the basis for determining longitudinal seismic stresses in the regulatory documents (Building Code) in the Commonwealth of Independent States countries (SNiP 2.05.06-85* (RF) and in Uzbekistan (KMK 2.01.03-96).

It is obvious that under seismic waves propagation in soil medium with embedded pipeline, the longitudinal strain of the pipeline cannot be equal to the soil strain, as it is assumed in [9].

As noted in [12–16], this method can estimate the upper limit of seismic stress in an underground pipeline. Calculations by this method [38] show that longitudinal stresses in underground steel pipelines, depending on ground conditions, reach values from 20 to 100 MPa. These values of longitudinal stresses do not exceed the tensile strength of steel pipe. This circumstance is corrected in [38] by introducing coefficient m_3, which is determined by formula

$$m_3 = \tau_{np} / \tau_3 , \quad (1)$$

where $\tau_{np} = f\sigma_N + c$,

f is the coefficient of internal friction in soil,

σ_N is normal stress, determined by the pipeline laying depth in soil,

c is cohesion force in soil,

τ_3 is shear stress at the pipe-soil contact.

The definition of τ_3 in [38] is proposed experimentally, which is associated with many difficulties.

In [38], a final value of longitudinal stress in the underground pipeline is estimated multiplying coefficient m_3, determined by this method, by the value of longitudinal stress. Due to the complexity of determining shear stress τ_3, this method of estimating longitudinal seismic stress in an underground pipeline has not found its wide application in practice. However, due to its simplicity, this method is still included into the regulatory documents of the CIS countries, without taking into account coefficient m_3.

The fact that the first method is based on an incorrect hypothesis on longitudinal strains equality of the pipeline and soil makes us look for other methods to determine longitudinal seismic stresses in an underground pipeline. As a result, the second method was proposed.

The second method for determining longitudinal seismic stresses in an underground pipeline was developed in [38]. This method is based on the hypothesis that a longitudinal seismic stress in an underground pipeline is generated by the interaction force at the pipe-soil contact, determined in the simplest case as

$$\tau = K_x u, \tag{2}$$

where τ is the force (shear stress) of interaction,

K_x is coefficient of longitudinal interaction,

u is relative displacement equal to $u = u_2 - u_1$;

u_1 is absolute displacement of soil particles,

u_2 is absolute displacement of pipeline particles (section).

In the general case, the values of u_1 and u_2, and, accordingly, u should be determined for each section of the pipeline, i.e. they are the variable values along the pipeline length. They also vary in time as seismic wave parameters and are the functions of time parameters t and coordinate x directed along the pipeline axis

$$u_1 = u_1(t, x), \quad u_2 = u_2(t, x), \quad u = u(t, x). \tag{3}$$

Relationship (2) in [13–16] is attributed to V.A. Florin (1938), and the ones in [10–12] to other researchers. Using the external surface force (2), solutions to a number of one-dimensional problems on the underground pipeline vibrations were obtained in [13–16], and longitudinal stresses in the pipeline were determined.

The second method was further developed in [38]. Here, when solving one-dimensional problems of underground pipeline longitudinal vibrations, seismic load is considered to be known and taken in the form of function $u_1 = u_1(t)$, i.e. the absolute soil displacement depends on time only. Such a simplification is equivalent to the fact that soil medium is a non-deformable body and moves as a rigid body. Obviously, this simplification is opposite to the hypothesis of the first method, where soil is considered a deformable medium.

In [1–4, 13–16], many complex problems on underground pipeline longitudinal vibrations were considered and solved, the statements of which were similar or close to the ones of the second method.

In [38], longitudinal stresses in the pipeline were determined from the solution of one-dimensional stationary problem of longitudinal plane seismic wave propagation in an elastic underground pipeline, using relationships (2), (3). In [38], the results of the first method are taken as the first approximation by solving the equations of pipeline longitudinal vibrations. In [38], the first method is referred to as a «static» method and criticized as an inaccurate one.

Further, the solution of the first method is taken as the basis for determining longitudinal stresses in soil. Then in [38], a dynamic coefficient is introduced, which specifies the value of longitudinal stress in underground pipeline. The value of dynamic coefficient n_D varies within n_D = 0.2–3. As a result, the range of longitudinal stresses obtained in [38] varies from 4 to 300 MPa, which is an inaccurate value.

Besides, the essence of dynamic coefficient n_D and the problem statement on seismic vibrations of underground pipelines were not revealed in [38]. A number of significant drawbacks of the second method were noted in [13–16]. The second method, as well as the first one, does not lead to a more accurate and reliable determination of longitudinal stresses in the underground pipeline. This circumstance led to the formulation of the third method.

The basics of the third method are given in [11]. In [11], longitudinal stress in an underground pipeline is determined from solving coupled wave problems. The third method includes the advantages of the first two methods. Since it is practically very difficult to determine experimentally the change in soil displacements $u_1 = u_1(t, x)$ on soil-pipeline contact surface, it is proposed to determine function $u_1 = u_1(t, x)$ based on the solution of the problem of seismic wave propagation in soil with embedded pipeline.

In this case, firstly, it becomes possible to take into account not only the elastic properties, but dissipative (viscous, plastic) properties of soil as well. Secondly, in this case, dynamic stress normal to the outer surface of the pipeline $\sigma_{ND}(t, x)$ becomes known along the pipeline length.

Obviously, the shear stress (friction) τ tends to Coulomb friction τ_{np} at increasing relative displacement u. It follows that coefficient K_x in (2) should depend on σ_N; the latter, in turn, consists of two components

$$\sigma_N = \sigma_{NS} + \sigma_{ND}, \tag{4}$$

where σ_{NS} is the static normal stress, determined by the pipeline laying depth in soil.

The fact that the value of σ_{ND} may be greater than σ_{NS}, significantly affects the stress state of underground pipeline. Essentially, the value of σ_{ND} varies in the range $-\sigma_{ND\max} \le \sigma_{ND} \le \sigma_{ND\max}$. This means that on the pipe-soil contact surface, the soil separation from the pipeline may occur.

In addition, in the second method, the direction of the interaction force is not explicitly taken into account (2). The sign τ can be precisely determined only from relation

$$\tau = \mathrm{sgn}(v) K_x(\sigma_N) u, \tag{5}$$

where $v = v_2 - v_1$, v_2 is the velocity of soil particles, v_1 – velocity of pipeline particles on the contact surface. Obviously, at $v < 0$, $\mathrm{sgn}(v) = -1$, and at $v > 0$, $\mathrm{sgn}(v) = +1$. The case at v = 0 is considered as a special case [11].

As is shown in [10], at critical value of $u = u_*$, soil separation from the pipeline occurs and the shear stress on the surface of their contact is determined from the Coulomb-Amontons law, i.e. in this case $\tau = \tau_{np}$. Experimental studies of the underground pipelines-soil interaction under static and dynamic loads in [11] show that in fact there is no clear boundary in the pipe-soil contact.

A certain contact layer of soil is involved in the interaction, the thickness of which depends on the outer diameter and the roughness of pipeline outer surface and on strain properties of the pipeline and soil, on disturbed or undisturbed soil structure.

As shown in [11], this contact layer of the pipeline-soil interaction is strained strongly – till the destruction. The soil beyond the contact layer may be strained elastically or non-elastically without destruction.

Further, taking into account all the above factors and equations (3)–(5), the problem of seismic wave propagation in a pipeline is solved and the longitudinal (seismic) stress is determined.

The third method, as you can see, is quite complicated. However, it is more accurate and reliable in contrast to the former ones [11, 12].

Thus, the development of the methods to determine longitudinal stresses led to the formulation of the third method. In this paper, longitudinal seismic stresses in an underground pipeline are determined by the third method. According to [11, 12], in the simplest case, when considering one-dimensional coupled problems on seismic waves propagation in soil and along the underground pipeline, the pipeline-soil interaction forces play a significant role. Therefore, we will consider this issue separately.

2.2. Models of underground pipeline-soil interaction

In essence, an interaction model is a pipeline response to seismic effects. Seismic load is transferred to the pipeline through soil. The soil is strained under seismic impact. Soil strains near the boundary of contact with the pipeline differ from the ones that occur far from this boundary [11, 12]. As a result, a contact soil layer is formed at this boundary. The existence of the contact soil layer is experimentally and theoretically shown in [11, 12]. In [11], various laws of strain of the contact layer are considered. In [12], the cases and limits of applicability of these interaction laws are discussed, which are, in essence, the laws of special strain of the contact layer.

Based on the results of experimental and theoretical studies [11, 12], the process of underground pipeline-soil interaction is most reliably described by equations

$$\text{at } \sigma_N > \sigma_N^*,\ 0 \le u \le u_*$$

$$\frac{d\tau}{K_{xD}(\sigma_N, I_S)dt} + \mu_S(\sigma_N, I_S, \dot{u})\frac{\tau}{K_{xS}(\sigma_N, I_S)} = \frac{du}{dt} + \mu_S(\sigma_N, I_S, \dot{u})u \tag{6}$$

$$\frac{du}{dt} \ge 0$$

$$\frac{d\tau}{K_{xR}(\sigma_N, I_S)dt} = \frac{du}{dt}, \quad \frac{du}{dt} < 0 \tag{7}$$

$$\text{at } \sigma_N > \sigma_N^*,\ u > u_*$$

$$\tau = f\sigma_N, \quad \frac{du}{d\tau} \ge 0 \tag{8}$$

$$\tau = 0, \quad \frac{du}{dt} < 0 \tag{9}$$

$$\text{at } \sigma_N \le \sigma_N^*, \ \tau = 0, \tag{10}$$

where K_{xD} is the variable coefficient of dynamic interaction (at $\dot{u} \to \infty$);

K_{xS} is variable coefficient of quasistatic interaction (at $\dot{u} \to 0$);

K_{xR} is variable coefficient of interaction during reverse pipeline motion relative to soil;

μ_S is variable shear viscosity of soil;

$\dot{u} = du/dt$ is pipeline displacement rate relative to soil;

$I_S = u/u_*$ is a parameter characterizing the structural destruction of the soil contact layer,

$0 \le I_S \le 1$, at I_S = 0 the soil contact layer or contact bonds between the outer surface of the pipeline and soil are not destroyed, and at I_S = 1 these bonds are completely destroyed;

f is coefficient of internal friction of soil;

σ_N^* is tensile strength of soil (hereinafter, the compressive stresses are assumed to be positive).

Parameter μ_S is related to shear viscosity coefficient η_S by relationship

$$\mu_S = K_{xD} K_{xS} \left[\left(K_{xD} - K_{xS} \right) \eta_S \right]. \tag{11}$$

Interaction functions K_{xD}, K_{xS}, K_{xR} determined from the results of experimental studies in [11] have the following form

$$K_{xD}(\sigma_N, I_S) = K_{xD}^*(\sigma_N) \exp\left[\alpha \left(1 - I_S \right) \right], \tag{12}$$

$$K_{xS}(\sigma_N, I_S) = K_{xS}^*(\sigma_N) \exp\left[\beta \left(1 - I_S \right) \right], \tag{13}$$

$$K_{xR}(\sigma_N, I_S) = K_{xDN}^*(\sigma_N) / \left(1 - I_S \right), \tag{14}$$

where K_{xD}^* and K_{xS}^* are the secant coefficients of dynamic and quasistatic interaction of disturbed soil with the pipeline at $u = u_*$;

K_{xDN} and K_{xSN} are initial values of the interaction coefficients;

α and β are dimensionless coefficients characterizing the degree of change in K_{xDN} and K_{xSN}.

For the disturbed (I_S = 1) contact soil layer from (12) and (13) we obtain

$$K_{xDN} = K_{xD}^* \exp(\alpha), \quad K_{xSN} = K_{xS}^* \exp(\beta). \tag{15}$$

It follows from (15) that

$$\beta = \alpha + \ln(\gamma_* / \gamma_N), \tag{16}$$

where $\gamma_* = K_{xD}^* / K_{xS}^*; \gamma_N = K_{xDN} / K_{xSN}$.

Based on experimental results [11] we get

$$K_{xS}^*(\sigma_N) = K_{NS} \sigma_N, \quad K_{xD}^*(\sigma_N) = K_{ND} \sigma_N. \tag{17}$$

In [11] it is stated that $\gamma_* \ge \gamma_N$, so

$$\begin{gathered} \beta \ge \alpha; \quad \mu_S^* = B\dot{u}/(\gamma_* u_*), \\ \gamma_* = \gamma_N + (\gamma_*^m - \gamma_N)(\dot{u}/C_S)^\kappa \\ \mu_S(\sigma_N, I_S, \dot{u}) = \mu_S^* \exp\left[\varphi \left(1 - I_S \right) \right], \end{gathered} \tag{18}$$

where γ_*^m is the limit value of γ_*,

κ and φ are the dimensionless coefficients.

In [11], at σ_N > 1 MPa, it is recommended to replace formula (8) with the following formula

$$\tau = \tau_0 + f\sigma_N \Big/ \left(1 + f\sigma_N \Big/ \left(\tau_* - \tau_0\right)\right), \tag{19}$$

where τ_0 is the cohesion force of the soil contact layer;

τ_* is the limiting value of the friction force, τ_* = 0.7–0.9 MPa.

The parameters of the interaction model $B, K_{NS}, fu, \gamma_*^m, \alpha, u_*, \kappa, \varphi$ considered in [11] are determined from experimental results and have the following values for loess soils of disturbed structure and for steel pipeline: $\gamma_N = 1.1$; $f = 0.5$; $K_{NS} = 100$ m^{-1}; $u_* = 3 \cdot 10^{-3}$ m; $\sigma_N^* = 0.15$ MPa; $\varphi = 0$; $\alpha = 3$; $\kappa = 0.1$; $\gamma_*^m = 10$; $B = 200$; $C_S = 100$ m/s; $\tau_0 = 0$.

As can be seen, the interaction model described by equations (6)–(19) is more complicated than the one described by (2). However, an account for such determining factors, as the interaction rate, disturbance of the soil contact layer, cohesion forces and internal friction of soil leads to such cumbersome equations. In the simplest cases, not considering these factors, one can use equations (2) and (8) with the corresponding conditions as a model of interaction.

The law of interaction (2) is often used [1–4, 12–16, 28] in longitudinal stress calculations of underground pipelines. It is considered that the coefficient of longitudinal interaction K_x, determined from the results of static experiments, takes into account the pipeline laying depth. However, in [12–16, 38], the fact that a further increase in relative displacement value in (2) leads to soil separation from the pipeline and the value of τ after separation does not depend on u, is not taken into account. The Coulomb Law (8) is satisfied at this stage of interaction.

In [11] it was shown that the second stage of interaction for loess soils of disturbed structure occurs at $u_* = 3 \cdot 10^{-3}$ m. Such relative displacements between the underground pipeline and soil during strong earthquakes are possible [38, 69]. So in calculations it is necessary to take into account the entire interaction process for $\tau(u)$. In this case, to avoid the break between dependences (2) and (8) at point $u = u_*$, it is necessary to express the interaction coefficient K_x depending on σ_N taking into account (4).

In this case, the law of interaction (2) takes the form [11]

$$\tau = K_{xS}\left(\sigma_N\right) u e^{\left[\beta\left(1 - I_S\right)\right]} \text{ at } \sigma_N > \sigma_N^*, \quad 0 \le u \le u_*, \quad \frac{du}{dt} \ge 0, \tag{20}$$

where function $K_{xS}(\sigma_N)$ is determined from relationship (17).

In this case, the entire interaction process is described by equations (20), (8)–(10), and the value of u_* can be determined from the relationship

$$u_* = f / K_{NS}. \tag{21}$$

In [38], the interaction law of a model analogous to Kelvin – Voigt one is used, which does not describe soil relaxation. However, due to its simplicity, a Kelvin – Voigt-type interaction model is often used in calculations. Given the above factors, the Kelvin-Voigt type interaction model has the form [11]

$$\tau = K_{xS}\left(\sigma_N, I_S\right) u + \eta_S\left(\sigma_N, I_S\right) \frac{du}{dt} \text{ at } \sigma_N > \sigma_N^*, \ 0 \le u \le u_*, \ \frac{du}{dt} > 0, \tag{22}$$

where $\eta_S\left(\sigma_N, I_S\right)$ is the soil shear viscosity coefficient, determined from relationships

$$\begin{gathered} \eta_S\left(\sigma_N, I_S\right) = \eta_S^*\left(\sigma_N\right) \exp\left(\alpha_S\left(1 - I_S\right)\right) \\ \eta_S^*\left(\sigma_N\right) = f\sigma_N / C_S, \ \ u_* = f\left(1 - \frac{du}{C_S dt}\right) / K_{ND}, \end{gathered} \tag{23}$$

where C_S is the shear wave propagation in soil. In this case the interaction process is described by equations (22), (8)–(10). $K_{xS}\left(\sigma_N, I_S\right)$ is determined from (13).

From relationships (23) it is seen that at $\frac{du}{dt} \to C_S,\ u_* \to 0;$ which does not correspond to reality. Nevertheless, interaction models (20) and (22) in simplified versions are widely used in calculating the underground pipelines strength under seismic loads.

The above analysis of the process and the laws of interaction show that they are quite complex. As will be shown below, longitudinal stress in an underground pipeline substantially depends on the correct choice of the interaction model.

2.3. The statement of the problem of longitudinal interaction of an underground pipeline with soil when exposed to plane seismic waves and the method to solve them

The problem of soil interaction with an underground pipeline laying on a certain depth from the surface is a three-dimensional one. With some simplifications it can be reduced to a two-dimensional problem. In these two cases, mathematical statement of the problem leads to complex partial differential equations describing the process of pipeline-soil interaction with many unknowns. Obtaining a solution to these equations is a rather laborious and complex mathematical problem.

With some more powerful simplifications, the problem can be reduced to one-dimensional problem. Consider an underground pipeline as an extended rod with an x axis, on the outer surface of which an interaction (friction) force τ acts, defined by equations (2) or (6)–(10) or (20). When using these equations to determine interaction force τ, it is necessary to know the absolute value of soil displacement u_1 as a function $u_1(t, x)$ and the dynamic pressure σ_{ND} normal to the outer surface of the pipeline as a function $\sigma_{ND}(t, x)$.

The value of σ_{NS} is determined by the pipeline laying depth in soil and is assumed constant over time and along the pipeline length. To determine the functions $u_1(t, x)$ and $\sigma_{ND}\left(t, x\right) = K_\sigma \sigma_2\left(t, x\right)$ (K_σ is the soil lateral pressure coefficient, σ_2 – longitudinal stress in soil), consider the soil medium around an underground pipeline as a cylindrical rod with a radius $R = H$, where H is the pipeline laying depth in soil, determined by the distance from the outer (day) soil surface to the pipeline axis x, which is also the axis of soil cylinder.

Initial sections $x = 0$ of the pipeline and soil coincide. Outer surface of the pipeline in contact with soil, in this case, is the surface of a cylindrical cavity with a diameter $D_B = D_H$, where D_H is the outer diameter of the pipeline inside soil cylinder. Soil medium can also be considered as a half-space with an x axis coinciding with the pipeline axis with a cylindrical cavity of diameter D_B along the x axis. In both cases, the one-dimensional motion of soil is described by the same equations.

At the section $x = 0$ (the initial section of the pipeline and soil), a load that generates a plane wave in soil half-space and the pipeline is defined by equations

$$\begin{gathered}\sigma = \sigma_{\max} \sin\left(\pi t/T\right),\ 0 \le t \le \theta, \\ \sigma = 0,\ \ t > \theta,\end{gathered} \tag{24}$$

where T is the half-time of load,

θ is load action time,

$\sigma_{\max}$ is load amplitude,

σ is longitudinal stress acting along the x axis.

Considered simplifications of the «soil medium-pipeline» system lead to a description of their motion under dynamic load (24) by equations

$$\begin{gathered}\rho_{0i} \frac{\partial v_i}{\partial t} - \frac{\partial \sigma_i}{\partial x} + \kappa_i \sigma_{\tau i} = 0 \\ \frac{\partial v_i}{\partial x} - \frac{\partial \varepsilon_i}{\partial t} = 0,\end{gathered} \tag{25}$$

where v_i is the particle velocity (mass velocity) of the pipeline and soil on the same section $x = x_i$;

ρ_{0i} is the initial density of the pipe and soil material;

$\kappa_1 = \mathrm{sgn}(v)$ for pipeline,

$\kappa_2 = -\mathrm{sgn}(v)$ for soil;

$v = v_2 - v_1$ is relative velocity;

$\sigma_{\tau i}$ is reduced friction force acting per unit length of the pipeline and soil; at i = 1 all parameters and variables of equation (25) refer to the pipeline, and at i = 2 – to soil.

Values of $\sigma_{\tau i}$ for the pipeline and soil are determined from relationship

$$\sigma_{\tau i} = 4D_{H1}\tau \Big/ \left(D_{Hi}^2 - D_{Bi}^2\right), \tag{26}$$

where τ is the interaction force (friction force) acting between the pipeline and soil;

D_{Hi} is outer diameters of the pipeline and cylindrical soil rod;

D_{Bi} is inner diameters of the pipeline and cylindrical soil rod; $D_{B2} = D_{H1}$.

In fact, the surface interaction force (friction) is reduced by equation (26) to volume force, which is a consequence of reducing the problem to a one-dimensional statement [10–16]. Equations (25) contains three unknown variables σ_i, ε_i and v_i, for the determination of which (25) it is closed by the laws of strain of the pipeline and soil in the form

$$\frac{\partial \varepsilon_i}{\partial t} + \mu_i \varepsilon_i = \frac{\partial \sigma_i}{E_{Di}\partial t} + \mu_i \frac{\sigma_i}{E_{Si}}, \tag{27}$$

where E_{Di} is the dynamic compression modulus;

E_{Si} is static compression modulus;

μ_i is volume viscosity parameter related to the volume viscosity coefficient η_i by the ratio

$$\mu_i = \frac{E_{Di}E_{Si}}{\left(E_{Di} - E_{Si}\right)\eta_i}. \tag{28}$$

Equation of state (27) is a model of a standard linear viscoelastic body that takes into account the creep and relaxation of deformable bodies. Note that the basis of the interaction law (6) is equation (27). To close the equation in the case of ground condition (i = 2), the elastic-viscoplastic law of soft soils strain proposed by G.M. Lyakhov, cited in [10], can be used.

Thus, the solution to the problem of underground pipeline-soil interaction under plane seismic waves generated by a load (24) is reduced to solving two systems of differential equations of a hyperbolic type for the pipeline (i = 1) and soil (i = 2) [10]. These systems of equations are connected through the law of interaction (6)–(10), by means of relation (26). As a result, we have coupled boundary value problems with boundary conditions at x = 0, relation (24) and $x = C_{0i}t$ at the wave front

$$\sigma_i = C_{0i}\rho_{0i}v_i, \;\; v_i = C_{0i}\varepsilon_i, \;\; C_{0i} = \left(E_{Di}/\rho_{0i}\right)^{1/2}, \tag{29}$$

where C_{0i} is the velocity of longitudinal wave propagation in the pipeline (i = 1) and soil (i = 2).

In the case of a load generating a wave (24), the jumps in stresses $\langle \sigma_i \rangle$, strains $\langle \varepsilon_i \rangle$, and particle velocities $\langle v_i \rangle$ are equal to zero and the boundary conditions (29) take the form

$$\langle \sigma \rangle = 0, \;\; \langle \varepsilon \rangle = 0, \;\; \langle v \rangle = 0 \;\text{ at }\; x = C_{0i}t. \tag{30}$$

Note that the front end of the pipeline can be load-free (24), later the pipeline receives motion only through the effect of the interaction force, determined by relations (6)–(10), (26).

The system of partial differential equations (25), (27) with boundary conditions (24), (30) is numerically solved. Equations (24), (27) are of hyperbolic type and have real characteristic relations, which have the form

$$\left.\begin{aligned}
&d\sigma_i - C_{0i}\rho_{0i}dv_i = -C_{0i}^2\rho_{0i}g_i\left(\sigma_i,\varepsilon_i\right)dt + \kappa_i C_{0i}\sigma_{\tau i}dt \ \text{ at } \ dx/dt = +C_{0i}\\
&d\sigma_i + C_{0i}\rho_{0i}dv_i = -C_{0i}^2\rho_{0i}g_i\left(\sigma_i,\varepsilon_i\right)dt - \kappa_i C_{0i}\sigma_{\tau i}dt \ \text{ at } \ dx/dt = -C_{0i}\\
&d\sigma_i - C_{0i}^2\rho_{0i}d\varepsilon_i = C_{0i}^2\rho_{0i}g_i\left(\sigma_i,\varepsilon_i\right)dt \ \text{ at } \ dx/dt = 0\\
&g_i\left(\sigma_i,\varepsilon_i\right) = \sigma_i/\eta_i - E_{Di}E_{Si}\left(\varepsilon_i - \sigma_i/E_{Di}\right)/\left[\left(E_{Di}-E_{Si}\right)\eta_i\right]
\end{aligned}\right\} \tag{31}$$

In contrast to [10], in equations (25) and (31) there is an additional term related to κ_i and so, these equations are nonlinear. The wave fronts in the pipeline and soil are the lines of weak discontinuity, hence at the front $\tau = 0$. This leads to linear equations of the wave fronts and characteristics in both media. The application of the method of characteristics to equations (25), (27) leads to ordinary differential equations (31). The application of numerical methods to the solution of ordinary differential equations increases the accuracy of solution when compared to their application in partial differential equations [10].

To increase the accuracy of solution [10], equations (31) are reduced to a dimensionless form through the relations

$$\left.\begin{aligned}
&x^\circ = \mu_1 x/C_{01}, \ \ t^\circ = \mu_1 t, \ \ \sigma_i^\circ = \sigma_i/\sigma_{\max}, \ \ v_i^\circ = v_i/v_{\max}\\
&\varepsilon_i^\circ = \varepsilon_i/\varepsilon_{\max}, \ \ v_{\max} = -\sigma_{\max}/C_{01}\rho_{01}, \ \ \varepsilon_{\max} = \sigma_{\max}/E_{D1}
\end{aligned}\right\} \tag{32}$$

In these dimensionless variables, basic equations take the form

$$\left.\begin{aligned}
&K_{\rho i}\frac{\partial v_i^\circ}{\partial t^\circ} + \frac{\partial \sigma_i^\circ}{\partial x^\circ} - \kappa_i\sigma_{\tau i}^\circ = 0\\
&\frac{\partial v_i^\circ}{\partial x^\circ} + \frac{\partial \varepsilon_i^\circ}{\partial t^\circ} = 0\\
&K_{\varepsilon i}\frac{\partial \varepsilon_i^\circ}{\partial t^\circ} + \kappa_{\varepsilon i}\kappa_{\mu i}\varepsilon_i^\circ = \frac{\partial \sigma_i^\circ}{\partial t^\circ} + \kappa_{\mu i}\gamma_i\sigma_i^\circ\\
&K_{\rho i} = \frac{\rho_{0i}}{\rho_{01}}, \ \ K_{Ci} = \frac{C_{0i}}{C_{01}}, \ \ K_{\varepsilon i} = \frac{E_{Di}}{E_{D1}}, \ \ K_{\mu i} = \frac{\mu_i}{\mu_1}\\
&K_{vi} = \frac{\rho_{0i}C_{0i}}{\rho_{01}C_{01}}, \ \ \gamma_i = \frac{E_{Di}}{E_{Si}}, \ \ \sigma_{\tau i}^\circ = \sigma_{\tau i}\frac{C_{01}}{\sigma_{\max}\mu_1}
\end{aligned}\right\} \tag{33}$$

boundary conditions in dimensionless variables take the form

$$\left.\begin{aligned}
&\sigma^\circ = \sin\left(\pi t^\circ/\mu_1 T\right), \ \ 0 \le t^\circ \le \mu_1\theta\\
&\sigma^\circ = 0, \ \ t^\circ > \mu_1\theta\\
&\sigma_1^\circ = 0, \ \ \varepsilon_1^\circ = 0, \ \ v_1^\circ = 0 \ \text{ at } \ x^\circ = t^\circ\\
&\sigma_2^\circ = 0, \ \ \varepsilon_2^\circ = 0, \ \ v_2^\circ = 0 \ \text{ at } \ x^\circ = K_{Ci}t^\circ
\end{aligned}\right\} \tag{34}$$

Characteristic relations take the form

$$\left.\begin{aligned}
&d\sigma_i^\circ + K_{vi}dv_i^\circ = K_{\mu i}\left(K_{\varepsilon i}\varepsilon_i^\circ - \gamma_i\sigma_i^\circ\right)dt^\circ + \kappa_i K_{Ci}\sigma_{\tau i}^\circ dt^\circ \ \text{ at } \ dx^\circ/dt^\circ = +K_{Ci}\\
&d\sigma_i^\circ - K_{vi}dv_i^\circ = K_{\mu i}\left(K_{\varepsilon i}\varepsilon_i^\circ - \gamma_i\sigma_i^\circ\right)dt^\circ - \kappa_i K_{Ci}\sigma_{\tau i}^\circ dt^\circ \ \text{ at } \ dx^\circ/dt^\circ = -K_{Ci}\\
&d\sigma_i^\circ - K_{\varepsilon i}d\varepsilon_i^\circ = K_{\mu i}\left(K_{\varepsilon}\varepsilon_i^\circ - \gamma_i\sigma_i^\circ\right)dt^\circ \ \text{ at } \ dx^\circ/dt^\circ = 0
\end{aligned}\right\} \tag{35}$$

In equations (33)–(35) at $i = 1$, $K_\rho = K_C = K_\varepsilon = K_\mu = K_v = 1$.

Equations (35) at boundary conditions (34) (at zero initial conditions) are solved numerically by the finite difference method in an implicit scheme. The difference equations for system (35) are similar to the equations

given in [10]. The difference is the presence in (35) of nonlinear terms related to the interaction force $\sigma^{\circ}_{\tau i}$. In contrast to [1], computer calculations are performed on two parallel characteristic planes $t^{\circ}x^{\circ}$ (Figure 1) (for the pipeline (i = 1) and for soil (i = 2). The axes t°, x° and grids of discrete points are similar.

The initial sections x° = 0 for both planes coincide. Boundaries confined by wave fronts are different. In the pipeline, the wave propagates along the line $x^{\circ} = t^{\circ}\,(K_{C1} = 1)$, and in soil – along the line $x^{\circ} = K_{C2}t^{\circ}\,(K_{C2} = C_{02}/C_{01} < 1,\ C_{02} < C_{01})$ (Figure 1).

The time Δt° and space Δx° steps are chosen from the Courant stability condition for this case.

$$\Delta x^{\circ} \geq K_{C1}\Delta t^{\circ} > K_{C2}\Delta t_{\circ}. \tag{36}$$

Condition (36) ensures that the characteristic lines on the calculated layer j do not go beyond the lines i–1 and i+1 (Figure 1) on which all wave parameters are considered known. On the line j + 1, the wave parameters are first determined in soil, then knowing the interaction force $\sigma_{\tau i}$, the wave parameters in the pipeline are calculated. There are three types of calculation points in each time layer j + 1, point 1 at the initial section, point 2 inside the area, point 3 at the wave front. The wave parameters at these points are calculated according to their calculation algorithms. At points 1 and 3, they are calculated with account for the boundary conditions (34).

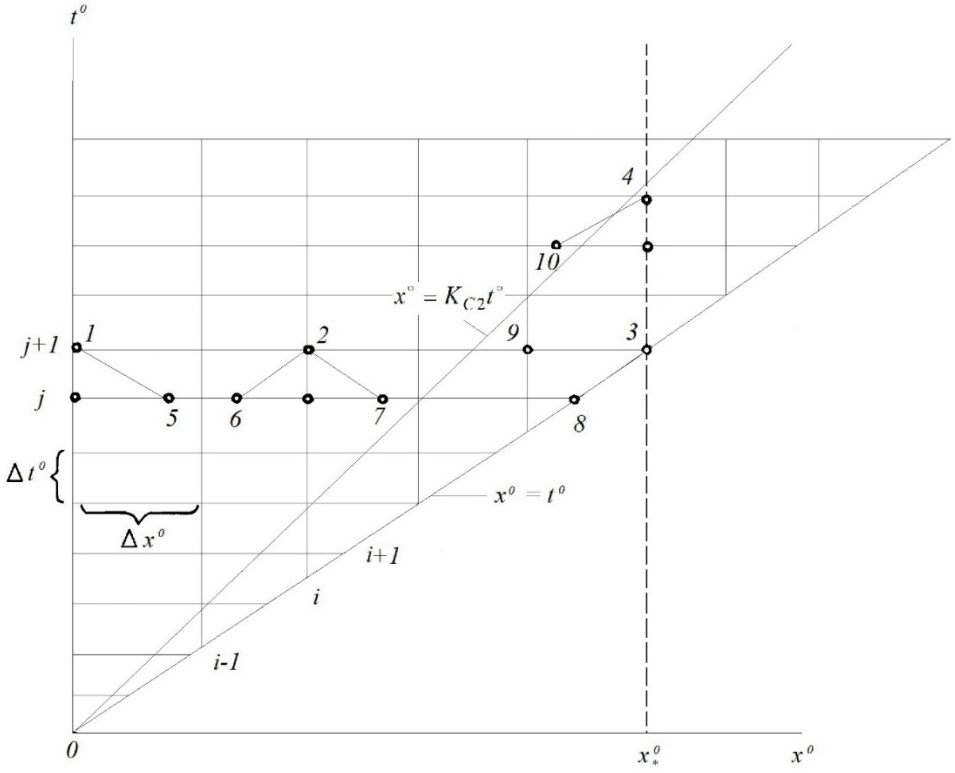

Figure 1. Sampling scheme on the characteristic planes of numerical solution.

At the intermediate points of type 9, the wave parameters are determined by interpolation method. The values of the known wave parameters in the time layer j at non-nodal points of 5, 6, 7 types are determined by interpolation too. In calculations, soil medium has an unlimited boundary. The wave front $x^{\circ} = K_{C2}t^{\circ}$ can extend to infinity. The pipeline may have a finite length $x^{\circ} = x^{\circ}_{*}$ or may have an infinite length (in calculations x°_{*} = 1 000 000.0). In the case of a finite length of the pipeline after the front has traveled the distance $x^{\circ} = x^{\circ}_{*}$, the boundary conditions at the final section of the pipeline are set in the form:

in case of a free end

$$\sigma^{\circ} = 0 \text{ at } x^{\circ} = x^{\circ}_{*} \tag{37}$$

in case of a fixed end

$$v^{\circ} = 0 \text{ at } x^{\circ} = x_{*}^{\circ}. \quad (38)$$

Based on the compiled algorithm, a program has been developed in Pascal algorithmic language and implemented in Delphi programming for calculating the wave parameters in the pipeline and soil, taking into account the interaction forces.

The reliability of the algorithm and computer program is proved by comparing the results of numerical solutions with the available experimental results on the underground pipeline-soil interaction under dynamic loading [11].

2.4. Reliability substantiation of the algorithm, program and numerical solutions

In the statement considered here, even for the simplest cases (elastic soil, elastic pipeline, with the law of interaction (2)), the problem has no analytical solution. Experimental studies of the underground pipeline-soil interaction in [4, 12–15, 38] were carried out under the iimpact of a static load on the pipeline. The soil in these cases remained undisturbed. In [11], field experiments were carried out, the statement of which coincides with the one considered in the paper. The difference lies in the fact that there the dynamic load was created by the explosion. The set-up and the diagram of the experiment are given in detail in [11].

The main objective of the experiment [11] was to determine the law of interaction of an underground pipeline with soil. In experiments, an asbestos-cement pipe of a length L = 3.9 m; D_{H1} = 0.32 m; D_{B1} = 0.28 m; C_{01} = 5000 m/s; γ_1 = 1.1; μ_1 = 10 000 s^{-1}; laying depth H = 1.7 m was used. Characteristics of loess soil were: volume density ρ_{02} = 1620–1760 kg/m^3 (in calculations ρ_{02} = 1700 kg/m^3); moisture content W = 18–21 %; C_{02} = 1000 m/s; K_{σ} = 0.3; γ_2 = 4; μ_2 = 100 s^{-1}.

Load characteristics (24), according to experimental data [11] were: $\sigma_{\max}$ 0.7 MPa, $T = \theta$ = 0.03 s.

The laws of interaction (6)–(10) and its characteristics are given in paragraph 2.2. In the experiment, the end of the pipeline was rigidly fixed. Therefore, condition (38) is satisfied at the end of the pipe as a boundary condition.

In the experiment in [11], the stresses generated by a plane blast wave were measured at the front and rear ends of the pipe, as well as the acceleration of the pipe and its displacement relative to soil and the stress normal to the outer surface of the pipe. The changes in shear stresses, relative displacements in time on the pipe contact surface with loess soil of a disturbed structure were determined according to the sensors records [11]; dependencies $\tau(u)$ were constructed.

A numerical solution program allows us to consider a problem in the statement similar to that of an experiment in [11]. Using the above initial experimental data [11], the changes of $u(t)$, $\tau(t)$ and $\tau(u)$ were obtained by numerical solution of a theoretical problem similar to the experiment based on the developed algorithm and software.

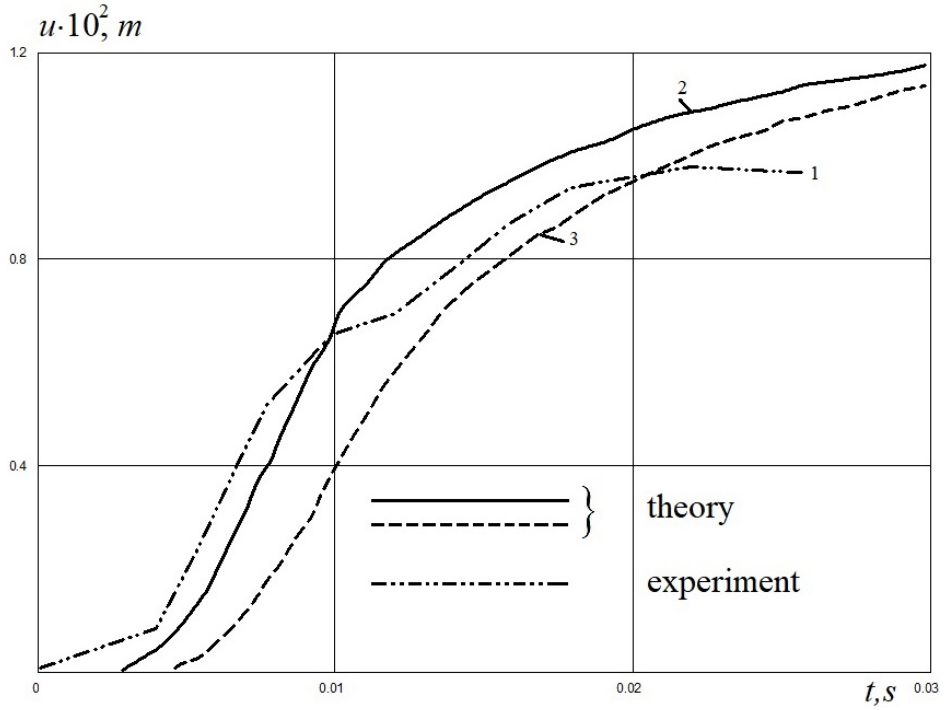

Figure 2. Change of relative displacement in time on the pipe-soil contact surface.

Comparison results of the numerical solution with the experiment are shown in Figures 2–4.

Figure 2 shows the changes in relative displacements in time. Curve 1 was obtained using the relative displacement sensor in the experiment [11] on a pipe section; the sensor was located at a distance of x = 3.625 m from the front end. Curves 2 and 3 were obtained by numerical solution and refer to the distances x = 1.95 m and 3.625 m, respectively, from the front end (initial section) of the pipe.

As seen from Figure 2, the results of calculations on a computer well agree with the experimental results (the scatter is 5–10 %).

Figure 3 shows similar comparisons of dependency $\tau(t)$. Here, curve 1 was obtained from the results of experimental measurements, and curves 2 and 3 – by numerical solution of a theoretical problem, the statement of which corresponds to the experimental statement. As seen from Figure 3, the experimental and theoretical curves coincide satisfactorily. Here, curves 2 and 3 relate to pipe sections at the distances of x = 1.95 m and 3.625 m from the initial section.

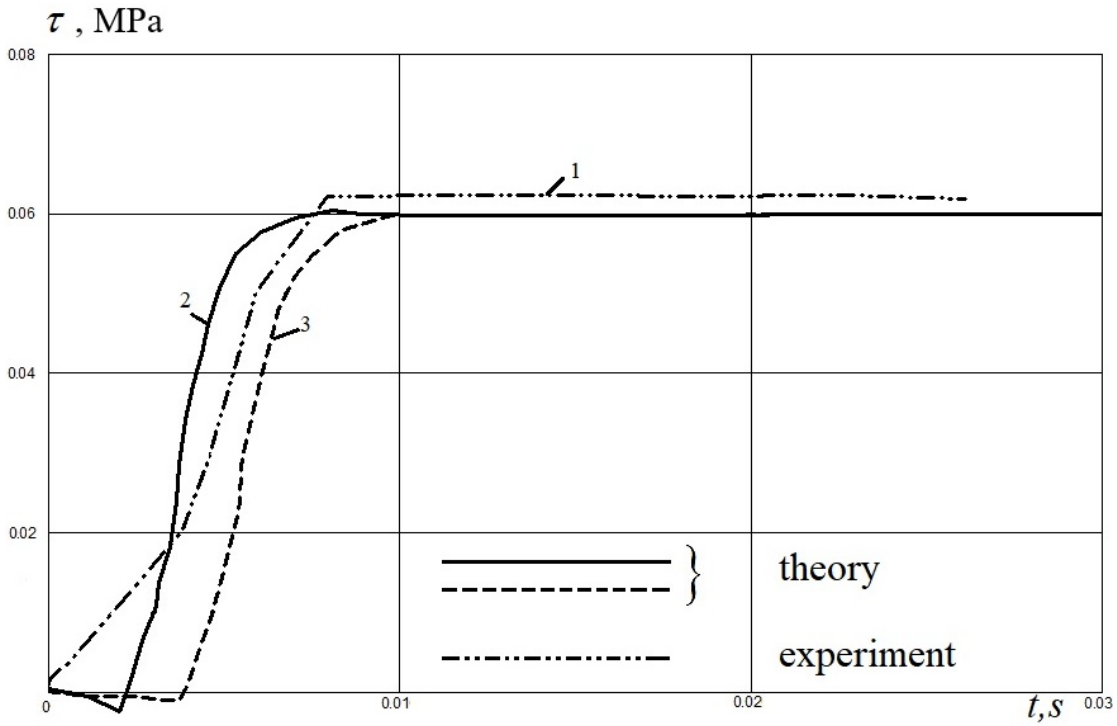

Figure 3. Change of shear stress in time on the pipe-soil contact surface.

Figure 4 shows a comparison of experimental and theoretical diagrams $\tau(u)$ plotted from dependences $\tau(t)$ and $u(t)$ in Figures 2 and 3. Due to the short length of the pipe (L = 3.9 m) theoretical dependences $\tau(u)$ are identical (curves 2,3) in its sections x = 1.95 m and 3.625 m, The coincidence of theoretical curves 2 and 3 at the initial stage of interaction, where the value of τ varies depending on u, with experimental one $\tau(u)$ is qualitatively satisfactory. Quantitatively, the scatter is 30–40 %. In the second section $\tau(u)$, where the pipe-soil slippage occurs, the agreement between experimental and theoretical results is good. Here the scatter is about 3 %.

In general, the agreement between experimental and theoretical diagrams $\tau(u)$ can be considered satisfactory (Figure 4). In the considered theoretical problem, one of the main components is the interaction law (6)–(10). A comparison of numerical solutions with the experiment, given in Figures 2–4, shows the reliability of the developed algorithms, computer programs and numerical solutions of the problem.

3. Results and Discussion

3.1. Longitudinal stresses in an underground pipeline in the case of an interaction model of the Hooke's law type

The interaction models considered above (6), (20), (22), are derived from the Hooke, Kelvin–Voigt laws, a law of a standard linear body for shear stresses and strains, respectively, [11]. So, they can be called the interaction models of the Hooke's, Kelvin-Voigt laws and the law of a standard body.

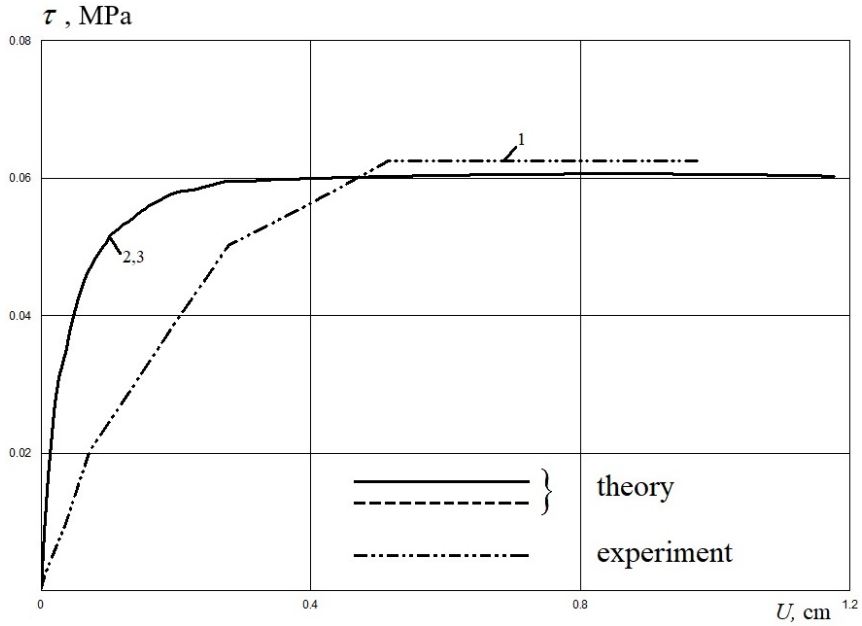

Figure 4. Theoretical and experimental diagrams of changes of shear stress on the pipe-soil contact surface.

In computer calculations, interaction models (6), (20) and (22) can be used separately or in combination with equations (7)–(10). In the case when interaction models (6), (20) and (22) between the pipeline and soil are used, excluding equations (7)–(10) and setting $\kappa_1 = \kappa_2 = 1$ in equation (25), an elastic or viscoelastic interaction force is obtained on the pipeline-soil contact surface.

At $\kappa_i = 1$, the force of interaction does not serve as the friction force. After the relative displacement reaches $u = u_{\max}$ or at $du/dt < 0$, the shear stress τ does not change the sign, but gradually decreases to zero and only at $u < 0$, $\tau < 0$. The case $\kappa_i = 1$ is applicable when the value of the relative displacement is small, i.e. $u << u_*$ and the structural bonds between the particles of the pipeline and soil are not broken; here the elastic forces act between them.

The developed algorithm and a program for numerical solution to the problem under consideration allow us to obtain results both for the case when an elastic (viscoelastic) bond is held between the pipeline and soil in the interaction process, and when this bond is not held on their contact surface. In the latter case, the force of interaction serves as the friction force.

The first case occurs when the structural bonds have been formed between the outer surface of the pipeline and soil; the bonds have a sufficient rigidity after the pipe has lain in soil for a long time. However, even in this case, at $u > u_*$, the contact layer of soil is destroyed and the pipeline separation from soil occurs; under longitudinal interaction, the interaction force serves as the friction force.

The second case occurs when the contact bonds are not formed between the pipe outer surface and soil (pipelines laid in soil of a disturbed structure) if the pipe-soil contact layer is disturbed (destroyed).

Consider the results of computer calculations obtained for the above cases when only condition (20) is satisfied between the pipeline and soil on their contact surface.

Let us start with the simplest case when the wave processes in soil surrounding the pipeline are not taken into account. In this case, in (4), $\sigma_{ND} = 0$, and σ_{NS} is approximately determined by the pipe laying depth

$$\sigma_{NS} = \gamma_{g2} H + \gamma_{g1} \pi \left(D_{H1}^2 - D_{B1}^2 \right) \Big/ 4 D_{H1}, \tag{39}$$

where γ_{g2} is the specific volume weight of soil,

γ_{g1} is specific volume weight of the pipeline material,

H is the pipeline laying depth.

The law of interaction (20) takes the form

$$\tau = K_{NS} \sigma_{NS} u e^{[\beta(1-I_S)]} \tag{40}$$

and is fulfilled at all values of u.

The initial data are: D_{H1} = 0.2 m; D_{B1} = 0.18 m; γ_{g1} = 780 кN/m^3; $\mu_1 = 10^4$ s^{-1}; C_{01} = 5000 m/s; H = 1 m; L = 1000 m; γ_{g2} = 200 KN/m^3; K_{NS} = 100 m^{-1}; $\sigma_{\max}$ = 0.5 MPa; T = 0.01 s.

Consider two calculation options at the above initial data: β = 2; κ = +1 and β = 0; $\kappa = \mathrm{sgn}(v)$. In the first option, the shear stress on the outer surface of the pipeline depends only on value of u. The structural bonds between the pipeline and soil are elastic ones and not broken at all values of relative displacement u. In the second option, the structural bonds between the soil particles and the outer surface of the pipeline are broken and the interaction force serves as the friction force. In this case, τ is determined from equations (40), (8)–(10). In these options, the relative displacement value is $u = u_1$, and u_2 = 0. The problems with similar statements are considered in [38].

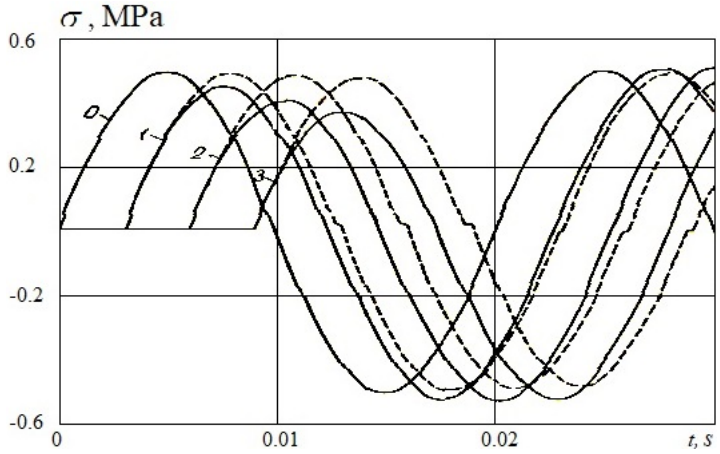

Figure 5. Changes of longitudinal stresses in the pipeline at x = 0; 15; 30; 45 m, not considering the wave processes in soil at $\sigma_N = \sigma_{NS} = const$ in the case of interaction model of Hooke's type.

Figure 5 shows the changes of longitudinal stresses related to these options. Here the solid curves are the calculations results of the first option, and the dashed curves – of the second option. Curves 0–3 refer to the distances x = 0; 15; 30; 45 m, respectively. Curves 0(x = 0) present the load given by the formula (24). In both options, the value of normal static soil pressure on the pipeline by formula (39) is equal to σ_{NS} = 0.023 MPa and is constant along the pipeline length.

As seen from Figure 5, the amplitudes of the load, set at the front end of the pipeline, remain constant over time (curves 0). The stress amplitudes in the next sections of the pipeline in both options vary differently (curves 1–3). In the first option (β = 2; κ = +1), the oscillations amplitudes of the first stresses decrease more noticeably in comparison with the second option ($\beta = 0$; $\kappa = \mathrm{sgn}(v)$). With an increase in time, this unloading decreases already in the next oscillations.

In both options, the relative displacement, i.e. the displacement of the pipeline relative to soil occurs only as a result of a steel pipe strain under longitudinal seismic stress of the amplitude of $\sigma_{\max}$ = 0.5 MPa. According to the data in [38], during 9 point magnitude earthquakes, longitudinal stresses in loess soils reach an amplitude of up to 0.5 MPa. Here, it is conditionally assumed that this load in the pipeline section x = 0 acts on the end of the pipeline. The change limits in shear stress and relative displacement are insignificant in the considered sections of the pipeline: in the first option: $-100 \le \tau \le 100$ Pa; $-6\cdot10^{-5} \le u \le 5\cdot10^{-5}$ m; in the second option: $-20 \le \tau \le 20$ Pa; $-8\cdot10^{-5} \le u \le 0$ m. Due to insignificant values of the relative displacement, and hence the shear stress, the amplitudes of longitudinal stresses along the pipeline practically do not change. A seismic stress wave of the amplitude of $\sigma_{\max}$ = 0.5 MPa does not affect significantly the pipeline in the considered options.

An increase in $\sigma_{\max}$ at x = 0 leads to similar results in Figure 5, with an increase in the stress amplitude in the pipeline cross sections.

Calculation results of considered options (Figure 5) show that it is impossible to determine and evaluate seismic stresses in the pipeline without account for the wave processes in soil. It follows that in the statement of the problem considered here and in similar problems [38], it is not possible to determine the longitudinal stresses in the pipeline not considering the wave processes in soil surrounding the pipeline. The results in Figure 5, of the changes in longitudinal stresses along the pipeline, correspond to the changes in wave parameters in viscoelastic rods [11]. This once again indirectly confirms the reliability of the obtained numerical solutions.

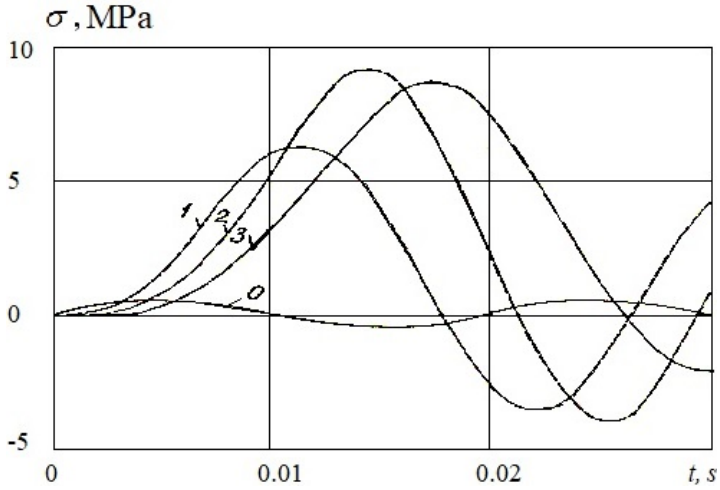

Figure 6. Change of longitudinal stresses in the pipeline at x = 0; 5; 10; 15 m, considering the soil movement at $\sigma_N = \sigma_{NS} = const$ in the case of interaction model of Hooke's type.

Now consider the change in longitudinal stresses in the pipeline taking into account wave processes in soil. Figure 6 shows the change of longitudinal stresses in the pipeline when a plane wave generated by the load (24) on section x = 0 of the pipeline and soil propagates through the soil surrounding the pipeline.

The characteristics of the pipeline, soil and load remained unchanged as in the case shown in Figure 5 (β = 2). Curves 0–3 in this case refer to distances x = 0; 5; 10; 15 m, respectively. In calculations, the soil pressure normal to the pipeline, determined by the pipe laying depth H = 1 m, remains along the entire length of the pipeline as in [38].

The dynamic component of normal pressure, σ_{ND}, i.e. $\sigma_N = \sigma_{NS} = const$ is not taken into account. When determining the longitudinal stress in the pipeline, only the soil displacement is taken into account, determined from the solution of equations (25), (27) at i = 2. Soil displacement values further enter equation (40) when determining the shear stress (interaction force) on the pipeline-soil contact surface.

Curve 0 in Figure 6 is the set load generating the wave. The amplitude of this load, $\sigma_{\max}$ = 0.5 MPa, remains constant over time. In the following sections x = 5; 10; 15 m (curves 1–3), the amplitudes of longitudinal stress increase significantly, from about 12 to 18 times, compared with the amplitude of $\sigma_{\max}$ = 0.5 MPa. This is due to soil displacement under wave propagation through it. Since the soil stiffness is approximately five times less (C_{01} = 5000 m/s; C_{02} = 1000 m/s) than the pipeline material, the soil displacement is significantly greater than the pipeline displacement as a result of their strain under the load (24).

As a result, the pipeline stress state actually determines the soil motion. Even in the case when the front end of the pipeline is load-free (24), the pattern in Figure 6 practically does not change, which confirms the significant and determinant role of soil medium in longitudinal stress formation in the pipeline. The value of relative displacement in the case shown in Figure 6 varies within $-0.5\cdot10^{-3} \le u \le 1\cdot10^{-3}$ m, and the value of shear stress varies within $-2\cdot10^{-2} < \tau < 2\cdot10^{-2}$ MPa. As seen, in this case, the values of relative displacement are an order of magnitude greater, and the values of shear stress are three orders of magnitude greater than in the previous case. In addition, in the case shown in Figure 5, the interaction force on the outer surface of the pipeline is always a passive resistance force, which leads to the wave amplitude attenuation over time.

In Figure 6, this interaction force due to the large strain in soil, hence, a greater displacement of soil relative to the pipeline, turns from a passive force into an active one. Under this active force, longitudinal stress in the pipeline increases too. The action of an active force occurs along the entire outer surface of the pipeline along its length. Therefore, the value of the interaction force dominates when comparing with the load at the front end of the pipeline. Due to this circumstance, the load (24) at the front end of the pipeline does not play a significant role at $\sigma_{\max}$ = 0.5 MPa. The results in Figure 6 are obtained at $u_* \to \infty$, i.e. in this case, equation (20) is used and not equations (7)–(10). Note that with the above values of the initial data, an account of equations (7)–(10) does not practically affect the change in longitudinal stresses (Figure 6).

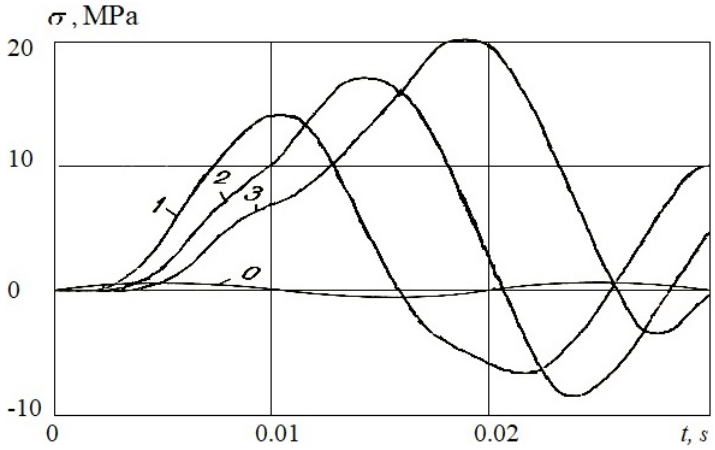

Figure 7. Change of longitudinal stresses in the pipeline at x = 0; 5; 10; 15 m, considering the soil movement at $\sigma_N = \sigma_{NS} + \sigma_{ND}$ in the case of interaction model of Hooke's type.

Consider the case of changes of longitudinal stresses in the pipeline with dynamic changes in the stress state of soil (Figure 7). In this case, the stress normal to the outer surface is $\sigma_N = \sigma_{NS} + \sigma_{ND} \neq const$ according to (4). The value of $\sigma_{ND} = K_\sigma \sigma_2 \left(t, x\right)$ is determined by longitudinal stress in soil $\sigma_2(t, x)$. Lateral pressure coefficient is K_σ = 0.3. The values of all other initial data of the problem remain unchanged. As seen from Figure 7, the amplitude of longitudinal stresses in comparison with the case at $\sigma_N = \sigma_{NS} = const$ (Figure 6), increases by two or more times. In Figure 7, just as in Figure 6, curves 0–3 relate to the distances from the initial section x = 0 (curve 0), x = 5; 10; 15 m (curves 1–3), respectively.

Calculations of longitudinal stresses for pipeline sections x = 30; 60; 90 m show that the amplitude $\sigma_{1\max}$ increases asymptotically. At x = 90 m, $\sigma_{1\max}$ = 27 MPa and in the next sections of the pipeline this value of longitudinal stress remains unchanged. An account of dynamic component of the normal stress leads to a three-time increase in longitudinal stresses in the pipeline, compared with the case when it is not taken into account. At the maximum stress in soil surrounding the pipeline, $\sigma_{2\max}$ = 0.5 MPa, longitudinal stress in the pipeline increases ($\sigma_{1\max}$ = 27 MPa) by 54 times.

In this case, the relative displacement and shear stress on the pipeline profile vary within $-1.5 \cdot 10^{-3} < u < 0$ m and $-2 \cdot 10^{-2} < \tau < 4 \cdot 10^{-2}$ MPa. Compared to Figure 6, the value of relative displacement is of the same order ($abs(u)$ = 1.5 · 10^{-3} m), and the value of shear stress, on account of the addition of σ_{ND}, increases by about 2 times. As a result, an increase in the pipeline longitudinal stress is three times greater in Figure 7 than in the case shown in Figure 6.

In the above options, the frequency of longitudinal waves in soil is taken as $f = 0.5T^{-1} = 50$ s^{-1}. Under low-frequency seismic loads, at f = 1–10 s^{-1}, the value of longitudinal stresses in the pipeline increases to 100 MPa or more. The determination of longitudinal stresses in the pipeline under low-frequency seismic wave propagation in soil is beyond the limits of this investigation.

3.2. Longitudinal stresses in an underground pipeline in the case of an interaction model of the Kelvin-Voigt law type

Consider the effect of laws (22) and (6) on the values of longitudinal stresses in the pipeline.

The interaction model (22) is constructed by analogy with the Kelvin – Voigt law [11]. In this case, the shear viscosity function $\eta_S(\sigma_N, I_S)$ is determined from relations (23). According to (23), the shear viscosity coefficient of disturbed soil on the underground pipeline-soil contact surface is determined by formula

$$\eta_S^* \left(\sigma_N\right) = f\, \sigma_N / C_S \,. \tag{41}$$

At the pipe laying depth H = 1 m, according to (39), σ_{NS} = 0.23 · 10^5 Pa. Taking the values of the coefficient of internal friction as equal to f = 0.5 and C_S = 500 m/s, we get τ_{np} = 0.115 · 10^5 Pa, η_S^* = 23 Pa·s/m.

The initial data for calculations in this case are K_{NS} = 100 m^{-1}; α_S = 1.2; β = 2; C_{01} = 5000 m/s; H = 1 m; T = 0.01 s; L = 1000 m; γ_{g1} = 780 kN/m^3; γ_{g2} = 200 kN/m^3; $\mu_1 = 10^4$ c^{-1}; D_H = 0.2 m; D_B = 0.18 m; C_S = 500 m/s; $\sigma_{\max}$ = 0.5 MPa.

The values of initial data for equation (40), in this case, are supplemented by the values of the parameters of equations (22), (23).

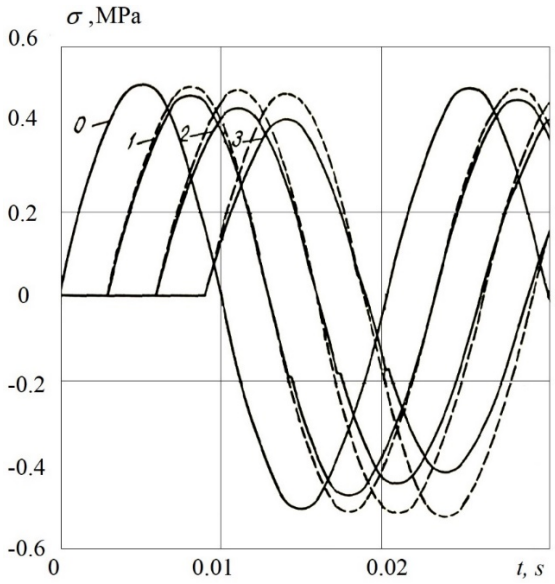

Figure 8. Change of longitudinal stresses in the pipeline at x = 0; 15; 30; 45 m, not considering the wave processes in soil at $\sigma_N = \sigma_{NS} = const$ in the case of interaction model of Kelvin-Voigt type.

First consider the case when the wave processes in the soil surrounding the underground pipeline are not taken into account β = 0; α_S = 0. This case corresponds to the linear law of interaction of the Kelvin-Voigt type. Calculation results are given in Figure 8 (dashed curves 0–3). Here, curve 0 is the set load at x = 0 changing according to equation (24). As seen from Figure 8, the wave amplitude at distances x = 15; 30; 45 m (dashed curves 1–3, respectively) attenuates slightly. In this case, the viscosity coefficient is η_S^* = 23 Pa·s/m.

Shear stress of the interaction τ determined by equation (22) varies within $-20 < \tau < 10$ Pa; relative displacement varies within $-8 \cdot 10^{-5} < u < 2 \cdot 10^{-5}$ m, i.e. these parameters are the same as in the case shown in Figure 5, at elastic interaction. Therefore, the change of stress over time at fixed sections of the underground pipeline is identical when using interaction models (20) and (22).

To identify the effect of shear viscosity of soil η_S^* on the stress state of an underground pipeline, the value of C_S in calculations was assumed to be artificially undervalued and equal to 0.5 m/s. The values of the remaining parameters did not change. Solid curves 1–3 in Figure 8 belong to this case. Here $\eta_S^* = 23 \cdot 10^3$ Pa·s/m, i.e. 1000 times more than in the former option. In this option, the amplitude of the first entry of longitudinal stress into the pipeline decreases by 10–15 % compared to the case when C_S = 500 m/s (dashed curves in Figure 8).

Weak effect of the viscous component of equation (22) is explained by small values of the relative displacement velocity du/dt ($-3 \cdot 10^{-2} < du/dt < 2 \cdot 10^{-2}$ m/s).

It follows that at an underground pipeline-soil interaction under seismic load, it is impossible to ignore the wave processes occurring in soil.

Consider the case of an underground pipeline-soil interaction according to model (22), taking into account the wave processes in soil medium. The initial data for the calculations are the same as in the former case (Figure 8, dashed curves).

First assume that $\sigma_N = \sigma_{NS} = const$, i.e. the pressure normal to the outer surface of the pipe along the entire length of the pipeline is considered as constant. The calculation results of this case are shown in Figure 9 in the form of graphs of change in longitudinal stress over time for sections x = 0; 15; 30; 45 m

(curves 0–3, respectively). In contrast to Figure 8, there is 1.2–2 times increase in stress amplitude in the pipeline sections. This is due to an increase in soil displacement relative to the pipeline caused by soil strain.

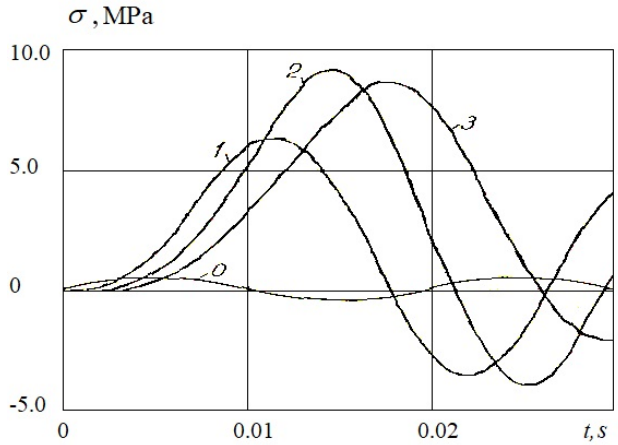

Figure 9. Change of longitudinal stresses in the pipeline at x = 0; 5; 10; 15 m, considering the wave processes in soil at $\sigma_N = \sigma_{NS} = const$ in the case of interaction model of Kelvin-Voigt type.

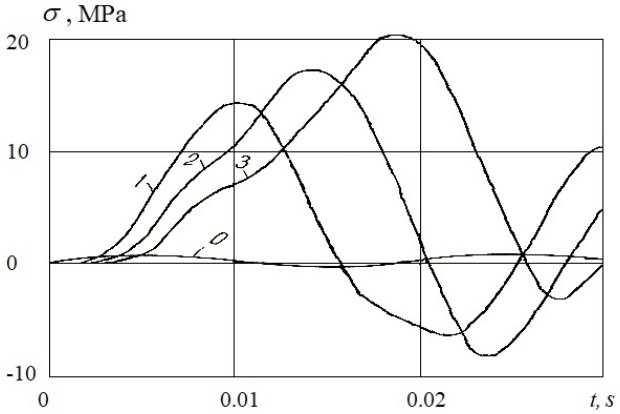

Figure 10. Change of longitudinal stresses in the pipeline at x = 0; 15; 30; 45 m, considering the wave processes in soil at $\sigma_N = \sigma_{NS} + \sigma_{ND}$ in the case of interaction model of Kelvin-Voigt type.

The values of relative displacement in this option of calculation vary within $-10^{-4} < u < 10^{-4}$ m, and the shear stresses vary within $-200 < \tau < 200$ Pa. As noted above, here a stress increase in the pipeline occurs due to the transformation of interaction force from a passive force into an active one.

An account for dynamic component of normal stress on the pipeline σ_{ND} leads to an even greater increase in longitudinal stress in the pipeline (Figure 10). In Figure 10, where $\sigma_N = \sigma_{NS} + \sigma_{ND} \neq const$ is taken in calculations, the longitudinal stress is doubled compared with the case shown in Figure 9, where $\sigma_N = \sigma_{NS} = const$.

However, the results obtained in calculations using the Hooke's type (Figures 5–7) and the Kelvin-Voigt type interaction models (Figures 8–10) are quantitatively identical. An account for shear viscosity of soil according to the Kelvin-Voigt model does not noticeably affect the maximum stress values. The results of calculations of longitudinal stresses in an underground pipeline in the case of the Hooke's type interaction model and in the case of the Kelvin-Voigt model are quantitatively and qualitatively identical (Figures 5–10).

3.3. Longitudinal stresses in an underground pipeline interacting with soil according to the model of a standard viscoelastic body

Consider the results of calculations of longitudinal stresses in an underground pipeline interacting with soil, taking into account the volume viscosity of soil. In this case, equation (6) is used as a model of interaction.

The initial data for the reference dependencies (8)–(18) and calculations are given above. For clarity, we will give them again: C_{01} = 5000 m/s; γ_{g1} = 780 kN/m^3; γ_N = 1.5; γ_*^m = 4; β = 2.5; φ = 1.2; K_{NS} = 100 m^{-1}; C_S = 500 m/s; T = 0.01 s; H = 1 m; D_H = 0.2 m; D_B = 0.18 m; L = 1000 m; $\sigma_{\max}$ = 0.5 MPa.

The results of computer calculations of longitudinal stresses in the pipeline, obtained only with equation (6) taken as the law of interaction, are shown in Figure 11. Curves 0–3 here relate to distances x = 0; 5; 10; 15 m, respectively. In this option of calculations, similar to the cases of the Hooke and Kelvin-Voigt types of interaction model the wave processes in soil are not taken into account at first. Curve 0 in Figure 11 refers to the change in stress at cross section x = 0 (initial section), i.e. this is a load generating a wave. As seen from Figure 11 at a distance of x = 5 m from the initial section, the amplitude of longitudinal stress decreases by ≈ 50 % (curve 1).

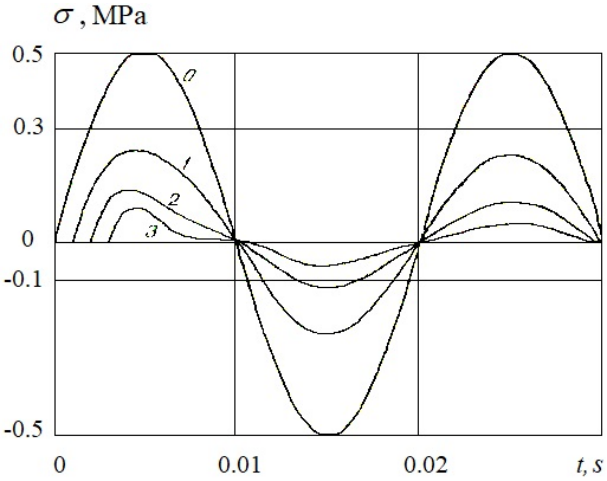

Figure 11. Change of longitudinal stresses in the pipeline at fixed values of x = 0; 5; 10; 15 m, not considering the wave processes in soil at $\sigma_N = \sigma_{NS} = const$ in the case of interaction model of a standard body type.

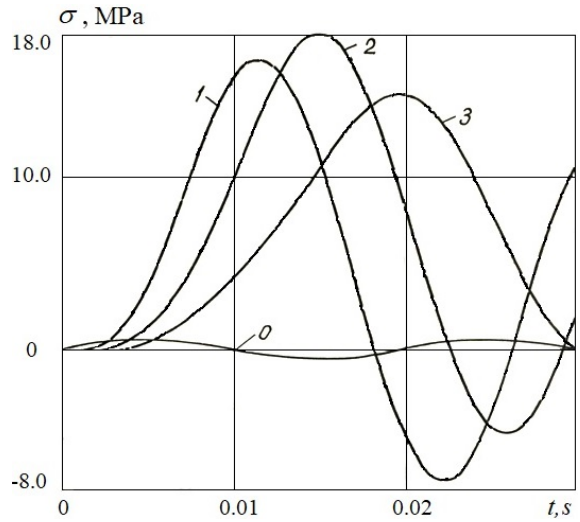

Figure 12. Change of longitudinal stresses in the pipeline at fixed values of x = 0; 5; 10; 15 m, not considering the wave processes in soil at $\sigma_N = \sigma_{NS} = const$ in the case of interaction model of a standard body type.

The stress in the subsequent sections of the underground pipeline at x = 10 and 15 m substantially attenuates (curves 2 and 3). Compared to the interaction models of the Hooke's and Kelvin-Voigt types, the stress wave attenuation along the underground pipeline is significant. This shows the effect of considering the volume viscosity of soil in the pipe-soil interaction. In this case, the stress amplitudes attenuate in subsequent stress fluctuations as well, which correspond to the results of known experiments [11].

The account of wave processes in soil medium according to the law of interaction (6) at $\sigma_N = \sigma_{NS} = const$ is shown in Figure 12. Curves 0–3 refer to the same sections of the underground pipeline x = 0; 5; 10; 15 m, respectively. Compared with the case when the laws of interaction of the Hooke's (Figure 6) and Kelvin-Voigt types (Figure 9) were used, a significant increase in the amplitude of longitudinal stresses is observed here. In all sections, the amplitudes of longitudinal stresses are almost two times higher than the results in Figures 6 and 9. This effect is further enhanced at $\sigma_N = \sigma_{NS} + \sigma_{ND} \neq const$ (Figure 13). An account for dynamic components of dynamic stress normal to the outer surface of the pipeline leads to 30–35 % increase in the amplitude of longitudinal stresses in the same sections x = 5; 10; 15 m from the initial section x = 0.

The results of calculations using the interaction model (6) of a standard body type show that in this case the change limits of the relative displacement $-4\cdot10^{-4} < u < 9\cdot10^{-4}$ m and shear stress $-65\cdot10^{3} < \tau < 60\cdot10^{3}$ Pa are greater than for the laws of interaction of the Hooke's and Kelvin-Voigt types.

In all cases, an account for the wave processes in the soil surrounding the underground pipeline by the changes in dynamic normal stress σ_{ND} and soil displacement u_2 leads to 40–50 times increase in the amplitude of longitudinal stress in the pipeline as compared with the amplitude of initial stress $\alpha_{\max}$ = 0.5 MPa.

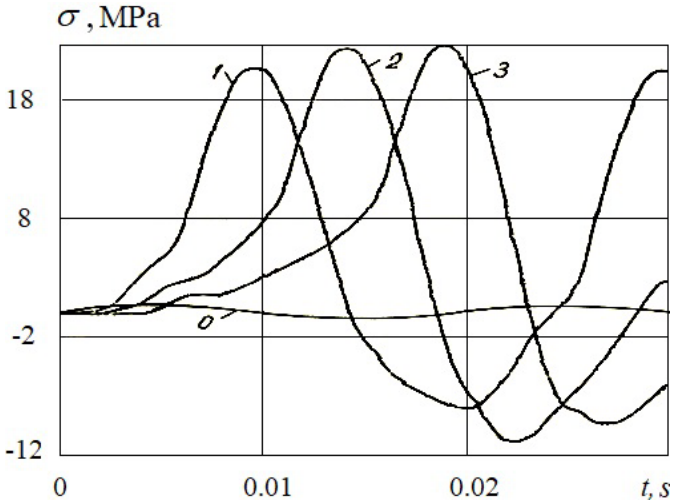

Figure 13. Change of longitudinal stresses in the pipeline at x = 0; 5; 10; 15 m, considering the wave processes in soil at $\sigma_N = \sigma_{NS} + \sigma_{ND}$ in the case of interaction model of a standard body type.

The greatest increase in the amplitude of longitudinal stress is observed in the case of using the law of interaction of a standard viscoelastic body type.

3.4. Longitudinal stresses in an underground pipeline interacting with soil according to a generalized interaction model

Changes in longitudinal stresses in the underground pipeline when using the law of generalized interaction (6)–(10) are shown in Figure 14. The values of the initial parameters remained the same as in Figure 13.

Here, curves 0–3 relate to sections x = 0; 5; 10; 15 m. In this case, the amplitude of longitudinal stresses in the pipeline is approximately 20 % less than in the case when only the interaction law (6) was used. This is explained by a decrease in the value of active shear stress – the interaction force in the case of the complete law (6)–(10).

According to estimated data [38], during the Gazli earthquake (1976), longitudinal stresses in underground gas pipelines amounted to σ_1 = 83.5–167.0 MPa. These values of longitudinal stresses are 3–7 times higher than the longitudinal stresses obtained above. However, the period of seismic wave vibrations in the Gazli earthquake was T = 0.5 s [38]. As noted above, the determination of longitudinal stresses for low-frequency seismic waves is considered separately.

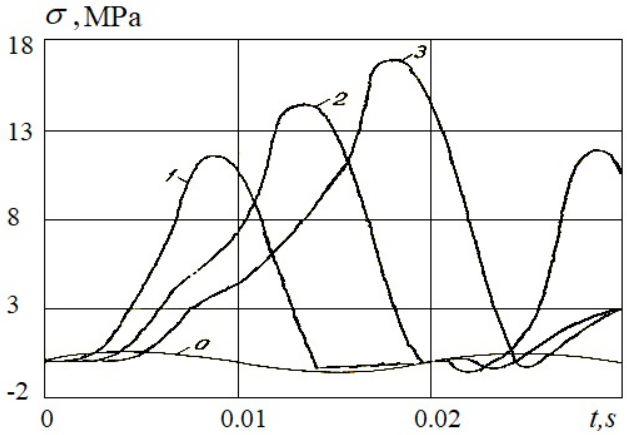

Figure 14. Change of longitudinal stresses in the pipeline at x = 0; 5; 10; 15 m, considering the wave processes in soil at $\sigma_N = \sigma_{NS} + \sigma_{ND}$ in the case of a generalized interaction model.

Thus, the values of longitudinal stresses in underground pipelines interacting with soil by various interaction laws and at the frequency of incident seismic wave f = 50 s^{-1} are given in this paper, with and without an account for the wave processes in soil medium.

4. Conclusions

1. The coupled wave problems of the underground pipeline-soil interaction under the influence of a seismic load were formulated taking into account the strain characteristics of the pipeline and soil and various laws of interaction.

2. For the numerical solution of the stated coupled wave problem, the method of characteristics with the subsequent application of the finite difference method in an implicit scheme was used. The chosen method of numerical solution and its advantages and disadvantages were substantiated.

3. An algorithm and program for solving numerical solution of coupled wave problems for an extended underground pipeline and for soil medium were compiled. Numerical solutions of test problems were obtained, the results of which were compared with experimental results and the reliability of the developed algorithms and a program for numerical solution of the problems under consideration were shown.

4. The analysis of the obtained numerical solutions, in the form of a change in longitudinal stresses in the underground pipeline, related to the statement of wave and dynamic theory of earthquake resistance of underground structures was carried out. The advantages and disadvantages of the considered theories were shown.

5. The results of calculations of longitudinal stresses in underground gas pipelines during the Gazli earthquake were considered and compared with the results of numerical solutions.

6. Longitudinal stresses of underground pipelines at their interaction with soil were determined according to non-linear laws of interaction of Hooke's type, Kelvin-Voigt type and a standard body. The advantages and disadvantages of the considered laws of interaction of underground pipelines with soil and their influence on the stress state of underground pipeline were shown.

7. The application of the developed method for calculating the stresses in underground pipelines improves the regulatory method by refining the KMK-2.01.03-96 (Building Code).

References

1. Muravyeva, L., Vatin, N. Risk Assessment for a Main Pipeline under Severe Soil Conditions on Exposure to Seismic Forces. Applied Mechanics and Materials. 2014. 635–637. Pp. 468–471. DOI: 10.4028/www.scientific.net/AMM.635-637.468.
2. Muravyeva, L., Vatin, N. The Safety Estimation of the Marine Pipeline. Applied Mechanics and Materials. 2014. 633–634. Pp. 958–964. DOI: 10.4028/www.scientific.net/AMM.633-634.958.
3. Muravyeva, L., Vatin, N. Application of the Risk Theory to Management Reliability of the Pipeline. Applied Mechanics and Materials. 2014. 635–637. Pp. 434–438. DOI: 10.4028/www.scientific.net/AMM.635-637.434.
4. Lalin, V.V., Kushova, D.A. New Results in Dynamics Stability Problems of Elastic Rods. Applied Mechanics and Materials. 2014. 617. Pp. 181–186. DOI: 10.4028/www.scientific.net/AMM.617.181.
5. Jung, J.K., O'Rourke, T.D., Argyrou, C. Multi-directional force–displacement response of underground pipe in sand. Canadian Geotechnical Journal. 2016. No. 11(53). Pp. 1763–1781. DOI: 10.1139/cgj-2016-0059.
6. Gao, F.-P., Wang, N., Li, J., Han, X.-T. Pipe–soil interaction model for current-induced pipeline instability on a sloping sandy seabed. Canadian Geotechnical Journal. 2016. No. 11(53). Pp. 1822–1830. DOI: 10.1139/cgj-2016-0071.
7. Wijewickreme, D., Monroy, M., Honegger, D.G., Nyman, D.J. Soil restraints on buried pipelines subjected to reverse-fault displacement. Canadian Geotechnical Journal. 2017. No. 10(54). Pp. 1472–1481. DOI: 10.1139/cgj-2016-0564.
8. Muravieva, L., Bashirzade, S. Behaviour underground pipelines laid in saturated soil. Russian journal of transport engineering. 2015. No. 3(2). DOI: 10.15862/01TS315.
9. Housner, G. Introduction to earthquake engineering, Second Edition, Shunzo Okamoto. ISBN 0–86008-361–6. University of Tokyo Press, 1984. 7–3-1 Hongo, Bunkyo-ku, Tokyo 113–91, Japan. 652 p. Earthquake Engineering & Structural Dynamics. 1985. No. 2(13). Pp. 278–278. DOI: 10.1002/eqe.4290130213
10. Sultanov, K.S., Loginov, P.V, Ismoilova, S.I., Salikhova, Z.R. Quasistaticity of the process of dynamic strain of soils. Magazine of Civil Engineering. 2019. 85(1). Pp. 71–91. DOI: 10.18720/MCE.85.7.
11. Sultanov, K.S., Bakhodirov, A.A. Laws of Shear Interaction at Contact Surfaces Between Solid Bodies and Soil. Soil Mechanics and Foundation Engineering. 2016. No. 2(53). Pp. 71–77. DOI: 10.1007/s11204-016-9367-7.
12. Bakhodirov, A.A., Ismailova, S.I., Sultanov, K.S. Dynamic deformation of the contact layer when there is shear interaction between a body and the soil. Journal of Applied Mathematics and Mechanics. 2015. No. 6(79). Pp. 587–595. DOI: 10.1016/j.jappmathmech.2016.04.005.
13. Israilov, M.S. Coupled seismic vibrations of a pipeline in an infinite elastic medium. Mechanics of Solids. 2016. No. 1(51). Pp. 46–53. DOI: 10.3103/S0025654416010052.
14. Georgievskii, D.V., Israilov, M.S. Seismodynamics of extended underground structures and soils: Statement of the problem and self-similar solutions. Mechanics of Solids. 2015. No. 4(50). Pp. 473–484. DOI: 10.3103/S0025654415040135.
15. Israilov, M.S. A new approach to solve the problems of seismic vibrations for periodically nonuniform buried pipelines. Moscow University Mechanics Bulletin. 2016. No. 1(71). Pp. 23–26. DOI: 10.3103/S0027133016010052.

16. Israilov, M.Sh. Analogiya lineynoy tsepochki i seysmicheskiye kolebaniya segmentnykh i vyazkouprugikh truboprovodov. Izvestiya Rossiyskoy akademii nauk. Mekhanika tverdogo tela. 2018. № 3. Pp. 119–128. DOI: 10.7868/S0572329918030121.
17. Liyanage, K., Dhar, A.S. Stresses in cast iron water mains subjected to non-uniform bedding and localised concentrated forces. International Journal of Geotechnical Engineering. 2018. No. 4(12). Pp. 368–376. DOI: 10.1080/19386362.2017.1282338.
18. Smith, A., Dixon, N., Fowmes, G. Monitoring buried pipe deformation using acoustic emission: quantification of attenuation. International Journal of Geotechnical Engineering. 2017. No. 4(11). Pp. 418–430. DOI: 10.1080/19386362.2016.1227581.
19. Meyer, V., Langford, T., White, D.J. Physical modelling of pipe embedment and equalisation in clay. Géotechnique. 2016. No. 7(66). Pp. 602–609. DOI: 10.1680/jgeot.15.T.024.
20. Feng, W., Huang, R., Liu, J., Xu, X., Luo, M. Large-scale field trial to explore landslide and pipeline interaction. Soils and Foundations. 2015. No. 6(55). Pp. 1466–1473. DOI: 10.1016/j.sandf.2015.10.011.
21. Matsuhashi, M., Tsushima, I., Fukatani, W., Yokota, T. Damage to sewage systems caused by the Great East Japan Earthquake, and governmental policy. Soils and Foundations. 2014. No. 4(54). Pp. 902–909. DOI: 10.1016/j.sandf.2014.06.019.
22. Lam, S.Y., Haigh, S.K., Bolton, M.D. Understanding ground deformation mechanisms for multi-propped excavation in soft clay. Soils and Foundations. 2014. No. 3(54). Pp. 296–312. DOI: 10.1016/j.sandf.2014.04.005.
23. Zhang, Z., Zhang, M. Mechanical effects of tunneling on adjacent pipelines based on Galerkin solution and layered transfer matrix solution. Soils and Foundations. 2013. No. 4(53). Pp. 557–568. DOI: 10.1016/j.sandf.2013.06.007.
24. Williams, E.S., Byrne, B.W., Blakeborough, A. Pipe uplift in saturated sand: rate and density effects. Géotechnique. 2013. No. 11(63). Pp. 946–956. DOI: 10.1680/geot.12.P.067.
25. Chatterjee, S., Randolph, M.F., White, D.J. The effects of penetration rate and strain softening on the vertical penetration resistance of seabed pipelines. Géotechnique. 2012. No. 7(62). Pp. 573–582. DOI: 10.1680/geot.10.P.075.
26. Sultanov, K.S. The attenuation of longitudinal waves in non-linear viscoelastic media. Journal of Applied Mathematics and Mechanics. 2002. No. 1(66). Pp. 115–122. DOI: 10.1016/S0021-8928(02)00015-1.
27. Sultanov, K.S., Khusanov, B.É. Determination of the slump-type settlement of a nonlinearly deformable soil mass during wetting. Soil Mechanics and Foundation Engineering. 2002. No. 3(39). Pp. 81–84. DOI: 10.1023/A:1020329100803.
28. Akimov, M.P., Mordovskoy, S.D., Starostin, N.P. Calculating thermal insulation thickness and embedment depth of underground heat supply pipeline for permafrost soils. Magazine of Civil Engineering. 2014. 46(2). Pp. 14–23. DOI: 10.5862/MCE.46.3.
29. Kalugina, J.A., Keck, D., Pronozin, Y.A. Determination of soil deformation moduli after National Building Codes of Russia and Germany. Magazine of Civil Engineering. 2017. 75(7). Pp. 139–149. DOI: 10.18720/MCE.75.14.
30. Mirsaidov, M.M., Sultanov, T.Z. Use of linear heredity theory of viscoelasticity for dynamic analysis of earthen structures. Soil Mechanics and Foundation Engineering. 2013. No. 6(49). Pp. 250–256. DOI: 10.1007/s11204-013-9198-8.
31. Mirsaidov, M.M., Sultanov, T.Z., Sadullaev, S.A. An assessment of stress-strain state of earth dams with account of elastic-plastic, moist properties of soil and large strains. Magazine of Civil Engineering. 2013. 40(5). Pp. 59–68. DOI: 10.5862/MCE.40.7.
32. Samarin, O.D. The temperature waves motion in hollow thick-walled cylinder. Magazine of Civil Engineering. 2018. 78(2). Pp. 161–168. DOI: 10.18720/MCE.78.13.
33. Loktionova, E.A., Miftakhova, D.R. Fluid filtration in the clogged pressure pipelines. Magazine of Civil Engineering. 2017. 76(8). Pp. 214–224. DOI: 10.18720/MCE.76.19.
34. Singh, M., Viladkar, M.N., Samadhiya, N.K. Seismic response of metro underground tunnels. International Journal of Geotechnical Engineering. 2016. No. 2(11). Pp. 1–11. DOI: 10.1080/19386362.2016.1201881.
35. Chernysheva, N.V., Kolosova, G.S., Rozin, L.A. Combined Method of 3d Analysis for Underground Structures in View of Surrounding Infinite Homogeneous and Inhomogeneous Medium. Magazine of Civil Engineering. 2016. 62(2). Pp. 83–91. DOI: 10.5862/MCE.62.8.
36. Lanzano, G., Bilotta, E., Russo, G., Silvestri, F. Experimental and numerical study on circular tunnels under seismic loading. European Journal of Environmental and Civil Engineering. 2015. No. 5(19). Pp. 539–563. DOI: 10.1080/19648189.2014.893211.
37. Chang, D.-W., Cheng, S.-H., Wang, Y.-L. One-dimensional wave equation analyses for pile responses subjected to seismic horizontal ground motions. Soils and Foundations. 2014. No. 3(54). Pp. 313–328. DOI: 10.1016/j.sandf.2014.04.018.
38. Erdik, M., Rashidov, T., Safak, E., Turdukulov, A. Assessment of seismic risk in Tashkent, Uzbekistan and Bishkek, Kyrgyz Republic. Soil Dynamics and Earthquake Engineering. 2005. No. 7–10(25). Pp. 473–486. DOI: 10.1016/j.sandf.2014.04.018.

Contacts:

Karim Sultanov, +998909702535; sultanov.karim@mail.ru
Jakhongir Kumakov, +998901765500; sultanov.karim@mail.ru
Pavel Loginov, +998909801765; lopavi88@mail.ru
Barno Rikhsieva, +998977750936; barno.khusanova@mail.ru

Инженерно-строительный журнал

ISSN 2071-0305

сайт журнала: http://engstroy.spbstu.ru/

DOI: 10.18720/MCE.93.9

Прочность подземных трубопроводов при сейсмических воздействиях

К.С. Султанов[a]*, Ж.Х. Кумаков[b], П.В. Логинов[a], Б.Б. Рихсиева[a]

[a] Институт механики и сейсмостойкости сооружений Академии наук Республики Узбекистан, г. Ташкент, Республика Узбекистан

[b] Ташкентский архитектурно-строительный институт, г. Ташкент, Республика Узбекистан

** E–mail: sultanov.karim@mail.ru*

Ключевые слова: прочность, сейсмостойкость, трубопровод, грунт, взаимодействия, механические свойства, численные методы, скорость деформации, напряжения

Аннотация. Приводится краткий анализ методов расчета на сейсмостойкость подземных трубопроводов, их преимущества и недостатки. Приведен анализ моделей взаимодействия подземных трубопроводов с грунтом при сейсмических (динамических) воздействиях. Поставлены связанные задачи о взаимодействии подземного трубопровода с грунтом при прохождении сейсмической волны в грунтовой среде, включающей трубопровод. Одномерные нестационарные волновые задачи для грунтовой среды и для трубопровода решены численно с применением метода характеристик и метода конечных разностей. Получены численные решения в виде изменения продольных напряжений по времени в различных сечениях трубопровода. Анализом полученных численных решений показана существенная зависимость значения продольных напряжений от волновых процессов в грунтовой среде и динамического напряженного состояния грунта, а также механических свойств грунта и материала трубопровода. Обнаружен фактор многократного возрастания продольного напряжения в подземном трубопроводе при его динамическом взаимодействии с грунтом. Показано, что главной причиной такого возрастания напряжения является динамическое напряженное состояние грунта вокруг трубопровода при его взаимодействии с грунтом. Полученные результаты являются основой для разработки нового нормативного расчета прочности подземных магистральных трубопроводов при сейсмических воздействиях.

Литература

1. Muravyeva L., Vatin N. Risk Assessment for a Main Pipeline under Severe Soil Conditions on Exposure to Seismic Forces // Applied Mechanics and Materials. 2014. 635–637. Pp. 468–471. DOI: 10.4028/www.scientific.net/AMM.635-637.468.
2. Muravyeva L., Vatin N. The Safety Estimation of the Marine Pipeline // Applied Mechanics and Materials. 2014. 633–634. Pp. 958–964. DOI: 10.4028/www.scientific.net/AMM.633-634.958.
3. Muravyeva L., Vatin N. Application of the Risk Theory to Management Reliability of the Pipeline // Applied Mechanics and Materials. 2014. 635–637. Pp. 434–438. DOI: 10.4028/www.scientific.net/AMM.635-637.434.
4. Lalin V.V., Kushova D.A. New Results in Dynamics Stability Problems of Elastic Rods // Applied Mechanics and Materials. 2014. 617. Pp. 181–186. DOI: 10.4028/www.scientific.net/AMM.617.181.
5. Jung J.K., O'Rourke T.D., Argyrou C. Multi-directional force–displacement response of underground pipe in sand // Canadian Geotechnical Journal. 2016. No. 11(53). Pp. 1763–1781. DOI: 10.1139/cgj-2016-0059.
6. Gao F.-P., Wang N., Li J., Han X.-T. Pipe–soil interaction model for current-induced pipeline instability on a sloping sandy seabed // Canadian Geotechnical Journal. 2016. No. 11(53). Pp. 1822–1830. DOI: 10.1139/cgj-2016-0071.
7. Wijewickreme D., Monroy M., Honegger D.G., Nyman D.J. Soil restraints on buried pipelines subjected to reverse-fault displacement // Canadian Geotechnical Journal. 2017. No. 10(54). Pp. 1472–1481. DOI: 10.1139/cgj-2016-0564.
8. Muravieva L., Bashirzade S. Behaviour underground pipelines laid in saturated soil // Russian journal of transport engineering. 2015. No. 3(2). DOI: 10.15862/01TS315.
9. Housner G. Introduction to earthquake engineering, Second Edition, Shunzo Okamoto. ISBN 0–86008-361–6. University of Tokyo Press, 1984. 7–3-1 Hongo, Bunkyo-ku, Tokyo 113–91, Japan. 652 p. // Earthquake Engineering & Structural Dynamics. 1985. No. 2(13). Pp. 278–278. DOI: 10.1002/eqe.4290130213
10. Султанов К.С., Логинов П.В., Исмоилова С.И., Салихова З.Р. Квазистатичность процесса динамического деформирования грунтов // Инженерно-строительный журнал. 2019. № 1(85). С. 71–91. DOI: 10.18720/MCE.85.7
11. Sultanov K.S., Bakhodirov A.A. Laws of Shear Interaction at Contact Surfaces Between Solid Bodies and Soil // Soil Mechanics and Foundation Engineering. 2016. No. 2(53). Pp. 71–77. DOI: 10.1007/s11204-016-9367-7.
12. Bakhodirov A.A., Ismailova S.I., Sultanov K.S. Dynamic deformation of the contact layer when there is shear interaction between a body and the soil // Journal of Applied Mathematics and Mechanics. 2015. No. 6(79). Pp. 587–595. DOI: 10.1016/j.jappmathmech.2016.04.005.

13. Israilov M.S. Coupled seismic vibrations of a pipeline in an infinite elastic medium // Mechanics of Solids. 2016. No. 1(51). Pp. 46–53. DOI: 10.3103/S0025654416010052.
14. Georgievskii D.V., Israilov M.S. Seismodynamics of extended underground structures and soils: Statement of the problem and self-similar solutions // Mechanics of Solids. 2015. No. 4(50). Pp. 473–484. DOI: 10.3103/S0025654415040135.
15. Israilov M.S. A new approach to solve the problems of seismic vibrations for periodically nonuniform buried pipelines // Moscow University Mechanics Bulletin. 2016. No. 1(71). Pp. 23–26. DOI: 10.3103/S0027133016010052.
16. Исраилов М.Ш. Аналогия линейной цепочки и сейсмические колебания сегментных и вязкоупругих трубопроводов // Известия Российской академии наук. Механика твердого тела. 2018. № 3. Pp. 119–128. DOI: 10.7868/S0572329918030121.
17. Liyanage K., Dhar A.S. Stresses in cast iron water mains subjected to non-uniform bedding and localised concentrated forces // International Journal of Geotechnical Engineering. 2018. No. 4(12). Pp. 368–376. DOI: 10.1080/19386362.2017.1282338.
18. Smith A., Dixon N., Fowmes G. Monitoring buried pipe deformation using acoustic emission: quantification of attenuation // International Journal of Geotechnical Engineering. 2017. No. 4(11). Pp. 418–430. DOI: 10.1080/19386362.2016.1227581.
19. Meyer V., Langford T., White D.J. Physical modelling of pipe embedment and equalisation in clay // Géotechnique. 2016. No. 7(66). Pp. 602–609. DOI: 10.1680/jgeot.15.T.024.
20. Feng W., Huang R., Liu J., Xu X., Luo M. Large-scale field trial to explore landslide and pipeline interaction // Soils and Foundations. 2015. No. 6(55). Pp. 1466–1473. DOI: 10.1016/j.sandf.2015.10.011.
21. Matsuhashi M., Tsushima I., Fukatani W., Yokota T. Damage to sewage systems caused by the Great East Japan Earthquake, and governmental policy // Soils and Foundations. 2014. No. 4(54). Pp. 902–909. DOI: 10.1016/j.sandf.2014.06.019.
22. Lam S.Y., Haigh S.K., Bolton M.D. Understanding ground deformation mechanisms for multi-propped excavation in soft clay // Soils and Foundations. 2014. No. 3(54). Pp. 296–312. DOI: 10.1016/j.sandf.2014.04.005.
23. Zhang Z., Zhang M. Mechanical effects of tunneling on adjacent pipelines based on Galerkin solution and layered transfer matrix solution // Soils and Foundations. 2013. No. 4(53). Pp. 557–568. DOI: 10.1016/j.sandf.2013.06.007.
24. Williams E.S., Byrne B.W., Blakeborough A. Pipe uplift in saturated sand: rate and density effects // Géotechnique. 2013. No. 11(63). Pp. 946–956. DOI: 10.1680/geot.12.P.067.
25. Chatterjee S., Randolph M.F., White D.J. The effects of penetration rate and strain softening on the vertical penetration resistance of seabed pipelines // Géotechnique. 2012. No. 7(62). Pp. 573–582. DOI: 10.1680/geot.10.P.075.
26. Sultanov K.S. The attenuation of longitudinal waves in non-linear viscoelastic media // Journal of Applied Mathematics and Mechanics. 2002. No. 1(66). Pp. 115–122. DOI: 10.1016/S0021-8928(02)00015-1.
27. Sultanov K.S., Khusanov B.É. Determination of the slump-type settlement of a nonlinearly deformable soil mass during wetting // Soil Mechanics and Foundation Engineering. 2002. No. 3(39). Pp. 81–84. DOI: 10.1023/A:1020329100803.
28. Акимов М.П., Мордовской С.Д., Старостин Н.П. Определение толщины теплоизоляции и заглубления подземного трубопровода теплоснабжения в многолетнемерзлых грунтах // Инженерно-строительный журнал. 2014. № 2(46). С. 14-23. DOI: 10.5862/MCE.46.3
29. Калугина Ю.А, Кек Д., Пронозин Я.А. Расчетные модули деформации грунта согласно национальным стандартам России и Германии // Инженерно-строительный журнал. 2017. № 7(75). С. 139–149. doi: 10.18720/MCE.75.14
30. Mirsaidov M.M., Sultanov T.Z. Use of linear heredity theory of viscoelasticity for dynamic analysis of earthen structures // Soil Mechanics and Foundation Engineering. 2013. No. 6(49). Pp. 250–256. DOI: 10.1007/s11204-013-9198-8.
31. Мирсаидов М.М., Султанов Т.З., Садуллаев Ш.А. Оценка напряженно-деформированного состояния грунтовых плотин с учетом упругопластических, влажностных свойств грунта и больших деформаций // Инженерно-строительный журнал. 2013. № 5(40). С. 59–68. DOI: 10.5862/MCE.40.7
32. Самарин О.Д. Распространение температурных волн в пустотелом толстостенном цилиндре // Инженерностроительный журнал. 2018. № 2(78). С. 161–168. doi: 10.18720/MCE.78.13
33. Локтионова Е.А., Мифтахова Д.Р. Фильтрация жидкости в засоренных напорных трубопроводах // Инженерно-строительный журнал. 2017. № 8(76). С. 214–224. doi: 10.18720/MCE.76.19
34. Singh M., Viladkar M.N., Samadhiya N.K. Seismic response of metro underground tunnels // International Journal of Geotechnical Engineering. 2016. No. 2(11). Pp. 1–11. DOI: 10.1080/19386362.2016.1201881.
35. Чернышева Н.В., Колосова Г.С., Розин Л.А. Пространственные расчеты подземных сооружений с учетом работы окружающего бесконечного массива в однородных и неоднородных областях комбинированным способом // Инженерно-строительный журнал. 2016. №2(62). С. 83-91. DOI: 10.5862/MCE.62.8
36. Lanzano G., Bilotta E., Russo G., Silvestri F. Experimental and numerical study on circular tunnels under seismic loading // European Journal of Environmental and Civil Engineering. 2015. No. 5(19). Pp. 539–563. DOI: 10.1080/19648189.2014.893211.
37. Chang D.-W., Cheng S.-H., Wang Y.-L. One-dimensional wave equation analyses for pile responses subjected to seismic horizontal ground motions // Soils and Foundations. 2014. No. 3(54). Pp. 313–328. DOI: 10.1016/j.sandf.2014.04.018.
38. Erdik M., Rashidov T., Safak E., Turdukulov A. Assessment of seismic risk in Tashkent, Uzbekistan and Bishkek, Kyrgyz Republic // Soil Dynamics and Earthquake Engineering. 2005. No. 7–10(25). Pp. 473–486. DOI: 10.1016/j.sandf.2014.04.018.

Контактные данные:

Карим Султанович Султанов, +998909702535; эл. почта: sultanov.karim@mail.ru

Жахонгир Хамзаевич Кумаков, +998901765500; эл. почта: sultanov.karim@mail.ru

Павел Викторович Логинов, +998909801765; эл. почта: lopavi88@mail.ru

Барно Бахтияровна Рихсиева, +998977750936; эл. почта: barno.khusanova@mail.ru